Frauenklinik der Technischen Universität München

Klinische Forschergruppe

Generation of integrin αvβ3 cytoplasmic and transmembrane domain mutants: characterisation of the impact of integrin conformation on human ovarian cancer cell proliferation

Leonora Petrova Brunie

Vollständiger Abdruck der von der Fakultät für Medizin der Technischen Universität München zur Erlangung des akademischen Grades eines Doktors der Medizin genehmigten Dissertation.

Vorsitzender: Univ.-Prof. Dr. E. J. Rummeny

Prüfer der Dissertation:

1. apl. Prof. Dr. U. Reuning
2. Univ.-Prof. Dr. B. Schmalfeldt

Die Dissertation wurde am 20.06.2012 bei der Technischen Universität München eingereicht und durch die Fakultät für Medizin am 26.09.2012 angenommen.

For my daughter Lara

Table of contents

List of abbreviations

% (v/v)	percent (volume)
% (v/w)	percent (weight)
AB	antibody
bp	base pair
BSA	bovine serum albumin
cDNA	complementary deoxyribonucleic acid
dH_2O	distilled water
DMEM	*Dulbecco´s Modified Eagle Medium*
DMSO	dimethyl sulfoxide
DNA	deoxyribonucleic acid
dNTPs	deoxynucleotide triphosphate
dsDNA	double-stranded deoxyribonucleic acid
E. coli	*Escherichia coli*
ECM	extracellular matrix
EDTA	ethylene diamine tetraacetic acid
EGF	epidermal growth-factor
EGF-R	epidermal growth-factor receptor
FCS	fetal calf serum
GpA	glycophorin A
h	Hour
Ig	immunoglobulin
kb	kilobase
mAB	monoclonal antibody
min	minute
mut	mutation
N-terminal	aminoterminal
OD	optical density
PCR	polymerase chain reaction
pH	potentia Hydrogenii
RGD	Arginine-Glycine-Aspartic acid
RNase	ribonuclease
RT	room temperature
sec	second
SD	standard deviation
TM	transmembrane
TMD	transmembrane domain
Tris	tris(hydroxymethyl)aminomethane
U	Unit
V	Volt
VEC	Vector
VN	vitronectin
WT	wild type

One- and three-letter amino acid code

A	Ala	alanine
C	Cys	cysteine
D	Asp	aspartic acid
E	Glu	glutamic acid
F	Phe	phenylalanine
G	Gly	glycine
H	His	histidine
I	Ile	isoleucine
K	Lys	lysine
L	Leu	leucine
M	Met	methionine
N	Asn	asparagine
P	Pro	proline
Q	Gln	glutamine
R	Arg	arginine
S	Ser	serine
T	Thr	threonine
V	Val	valine
W	Trp	tryptophan
Y	Tyr	tyrosine

1 Introduction

1.1 The integrin family

Organ development, haemostasis, tissue repair, angiogenesis, and immune response, are all biological mechanisms depending on cellular communications which occur due to a large number of various mediators including soluble and cell surface proteins. Some cell surface proteins permit the transmission of signals from extracellular to intracellular. One of the major cell surface protein families involved in all of these cell tasks is the superfamily of integrins (Anthis et al., 2009, 36700-36710, Bunch, 1841-1849).

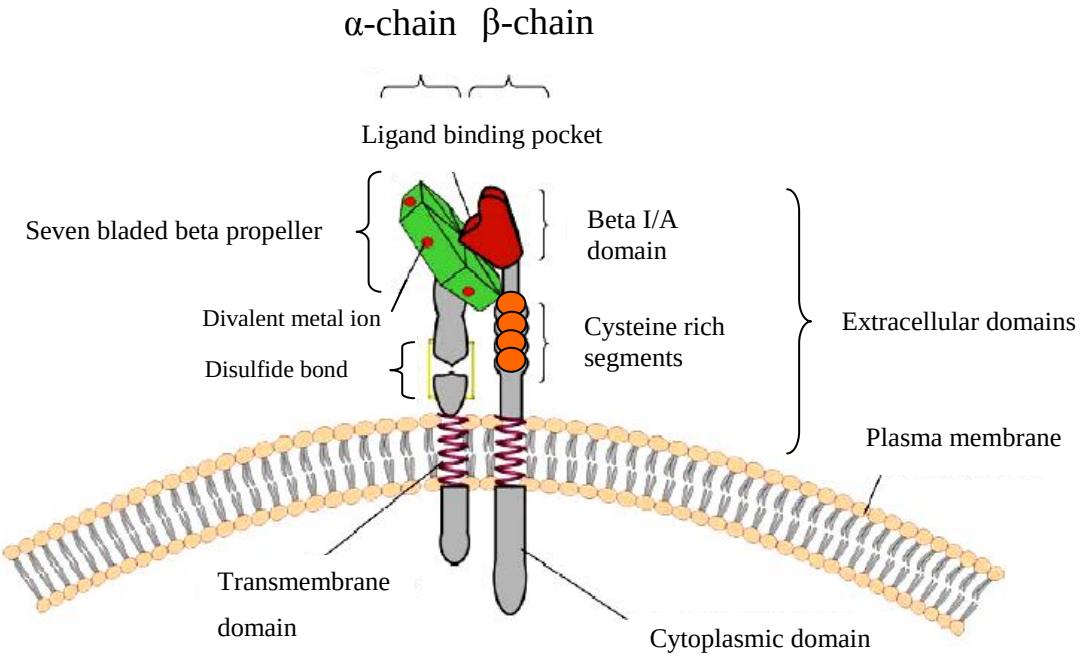

Figure 1 Scheme of an integrin molecule
Integrins are heterodimeric molecules comprised of an α- and a β-chain. Both chains contain a large extracellular domain, a single spanning transmembrane domain, and a short cytoplasmic region. The extracellular domain shows a high cysteine content in four tandem repeat regions (orange) in the integrin β-chain and a disulfide-bond in the integrin α-chain. The integrin α-chain has regions of homologue repeats, containing four divalent cation binding sites near its N-terminus (red dots). The α/β-heterodimer is a type I transmembrane protein with a large N-terminal extracellular domain forming the ligand binding site by interaction between both chains (Horton, 1997, 721-725). (Figure adapted from Bosserhoff, 2006, 963-975).

This protein family was given the name integrins by Hynes in 1986 to emphasise its role in integrating the intracellular cytoskeleton with the extracellular milieu (Horton, 1997, 721-725). Those heterodimeric cell-surface proteins mediate collectively cell-cell, cell-extracellular matrix (ECM) interactions in a wide range of physio- and pathophysiological situations (Travis et al., 2003, 192-197).

Integrins are adhesion receptor proteins on the cell surface. They are type I transmembrane glycoproteins, formed by two non-covalently associated chains, α- and β-subunits (Figure 1). Both chains contain a large extracellular domain, a single spanning transmembrane domain, and a relatively short cytoplasmic region (Humphries, 2000, 311-339). 18 α- and 8 β-integrin subunits are known to dimerise such that 24 different heterodimers are formed (Figure 2). Each of the 24 integrin heterodimers appears to have a specific function linked to their respective ligand binding specificity and signaling response.

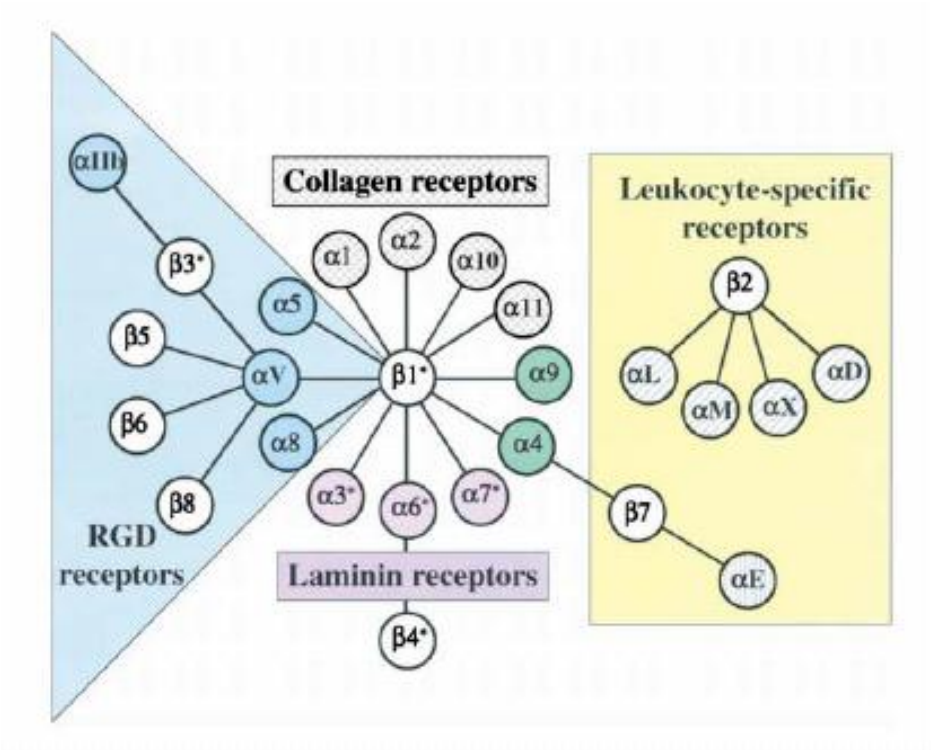

Figure 2 Superfamily of the integrin receptors
Integrins are α/β heterodimers. Currently 18 α- and 8 β-subunits are known. These α/β-subunits associate in a multitude of combinations forming 24 distinct integrin heterodimers. Each of the 24 heterodimers can be classified into several subfamilies according to their respective ligand binding specificity: integrins that recognise the RGD motif (blue), laminin-binding integrins (pink), collagen receptors (gray), and the leukocyte-specific receptors (yellow) (Hynes, 2002, 673-687). (Figure adapted from Hynes, 2002, 673-687).

One of the particularities of integrins is that they are capable of signal transmission across the plasma membrane in both directions, so called “outside-in” and “inside-out” signaling. There are several models discussing how integrins transmit signals from their extracellular ligand binding sites and their cytoplasmic domains (Xiong et al., 2001, 339-345, Gottschalk et al., 2002, 1800-1812, Takagi et al., 2002, 599-511, Luo and Springer, 2006, 579-586, Gahmberg et al., 2009, 431-444). However, the exact mechanism of integrin activation, the concominant conformational changes, and the transmission of signals through the membrane are still a matter of debate and an attractive challenge in protein science.

1.2 Integrin-mediated signaling

Integrins are bidirectional signaling receptors, they transmit signal information into and out of the cell. “Inside-out” signal transmission is a multiple step process in which the ligand binding affinity of integrins to ECM proteins depends on intracellular activation and cytoskeletal remodeling. This mechanism is associated with the binding of different intracellular ligands to the cytoplasmic domain of the integrin receptor, such as the talin head domain, p-paxillin, β-endonexin, cytohesin, calcium- and integrin-binding protein (CIB) (Calderwood, 2004, 657-666, Harburger and Calderwood, 2009, 159-163). The current model proposes that such events lead to unclasping of the cytoplasmic interface (Anthis and Campbell, 2011, 191-198). Hence, integrin transmembrane domain (TMD) interactions can be disrupted, and the orientation between the integrin α- and β-subunits might be interchanged (Humphries, 2000, 311-339). This allows legs extension of the extracellular domain and increases ligand binding affinity. Thus, conformational rearrangements switch the integrin from a low-affinity state (closed conformation) to a high-affinity state (open conformation) (Calderwood, 2004, 657-666). Integrins are activated and the outside-in signaling can be realised.

The “outside-in” signaling transmits signals to the cell interior. This mechanism is dependent on the binding of ligands to the integrin extracellular domain. According to the composition of the ECM, integrins activate one or more intracellular signaling pathways, including protein phosphorylation and cytoskeletal reorganisation (Vinogradova et al., 2002, 587-597). This complex network of signaling pathways initiated by integrins permits cells to survive, migrate, proliferate, and/or differentiate (Giancotti, 1997, 691-

700, Watt, 2002, 3919-3926, Al-Jamal and Harrison, 2008, 81-101, Morgan et al., 2009, 731-738).

As described above, integrins play diverse and important roles in most cell biological processes (Hynes, 2002, 673-687). Migration, adhesion, proliferation, differentiation, or cell apoptosis are important integrin functions in cell physiology. Disrupting the equilibrium between those tasks can provoke malignant uncontrolled cell proliferation, cancer development, tumor progression, and metastatic tumor cell dissemination. Thus, integrins are known to play a key role in pathophysiological processes, such as angiogenesis which is significant for tumor cell survival and growth and metastasis. However the precise mechanisms of tumor progression via integrins are still rather elusive. A large number of integrins are known to contribute to tumor progression, one among those is the integrin αvβ3 (Desgrosellier, 2010, 9-22). Integrin αvβ3 was found to be an important marker for tumor angiogenesis. Hence, integrin αvβ3 was observed to play a critical role in the progression and proliferation of certain types of cancer, such as colorectal cancer, glioblastoma, melanoma, breast, and ovarian cancer (Albelda et al., 1990, 6757-6764, Bello et al., 2001, 380-389, Hapke et al., 2001, 26340-26348, Hapke et al., 2003, 1073-1083, Vellon et al., 2005, 3759-3773, Le Tourneau et al., 2007, 21-24, Veeravagu et al., 2008, 7330-7339). However the multi-faceted role of integrin αvβ3 in the development, progression, and metastasis of cancer is not yet fully understood.

1.3 Integrin αvβ3

Integrin αvβ3 is one of the best characterized integrins; it was first purified from placenta by Pytela and co-workers in 1985, cloned, and sequenced by Suzuki in 1986 (Horton, 1997, 721-725). Integrin αvβ3 was termed “vitronectin receptor” as it preferably bind the plasma protein vitronectin (VN). However, the authors later found out that this term was not correct, since integrin αvβ3 was not selective for VN. The name integrin was given by Hynes et al. in 1986 (Tamkun et al., 1986, 271-282).

Integrin αvβ3 was found to have high expression levels in bone resorbing cells, and osteoclasts. Lower expression levels were detected in platelets and megakaryocytes, kidney, vascular smooth muscle, entothelium, and placenta. This multimodal expression of the integrin αvβ3 in normal tissues indicates its important role in organ development. However, integrin αvβ3 was found as well to be upregulated in certain other

pathophysiological events, such as cancer development, tumor progression, angiogenesis, and metastasis (Horton, 1997, 721-725). In that regard, Hapke and co-workers evaluated the impact of integrin αvβ3 on ovarian cancer cell biology (Hapke et al., 2003, 1073-1083). It was observed that the human ovarian cancer cell line OV-MZ-6 overexpressing αvβ3 and interacting with its major ligand VN displayed increased cell adhesion, motility, and proliferation. All of these cell biological functions are responsible for high malignancy and progression of ovarian cancer.

In Europe and the United States, ovarian cancer is the second most common malignant disease of the female reproductive system within all gynecological cancer diseases, with the highest mortality rate. Its etiology is still rather unclear. Several risk factors such as, age, infertility, nulliparity, and inherited genetic abnormality seem to be important in the ovarian cancer development. Some factors are also known to be protective, such as the number of pregnancies and the duration of intake of contraceptives. Most of the symptoms are unspecific and the patients cannot associate them to the development of a serious disease. For this reason, its diagnosis arises in the majority of cases in an advanced stage. This late diagnosis makes the therapy difficult and still unsatisfying. The combination of radical surgical debulking and chemotherapy is very aggressive and the remission times are often followed by recurrences. Therefore, several studies investigate new and more efficient treatments.

Unfortunately, the precise mechanism of tumor progression promoted via integrin αvβ3 has not yet been completely elucidated. Studies support its potential role in tumor progression mediated through signal transduction and its cooperation with other receptors known to be involved in cancerogenesis (Hapke et al., 2003, 1073-1083, Lössner et al., 2008, 2746-2761, Desgrosellier, 2010, 9-22). Due to their particular bidirectional signaling mechanism, the unravelling of integrin signal transduction pathways is an attractive challenge in protein science. This bidirectional signaling across the plasma membrane is in part materialised through dynamic conformational changes of the two integrin chains. However, in order to better understand the different conformational states of integrin receptors as they are presently understood, knowledge of its structure and function is important.

1.3.1 Structure of integrin αvβ3

The integrin αv-chain consists of 1018 amino acids with 13 potential N-linked glycosylation sites and four typical N-terminal repeat motifs. The integrin β3-chain is shorter (762 amino acids), less glycosylated, and contains four tandem repeats with a high cysteine content (Figure 1) (Horton, 1997, 721-725).

The crystal structure of integrin αvβ3 extracellular domain had been previously solved by Xiong and co-workers (Xiong et al., 2001, 339-345). Both extracellular integrin α- and β-subunits were found to present an ovoid protein head forming the ligand binding domain followed by two parallel tails. The extracellular head part of integrin β3 consists of a βA-domain and an immunoglobulin (Ig)-like hybrid domain. The integrin β3 tail consists of a PSI-(Plexine, Semaphorine, and Integrin), four epidermal growth factor (EGF)-like, and a β-tail-domain. The extracellular head part of the integrin αv-subunit consists of a seven-bladed β-propeller followed by a Ig-like *thigh*-domain connected through a *genu* to two *calf*-domains. Interestingly, this *genu* domain permits the integrin α- and β-tails to fold back at a ~135° angle, forming a V-shaped structure (Figure 3). The high degree of flexibility in the *genu* region is thought to be important for integrin activation and ligand binding affinity. The dynamic rearrangements of integrins will be explained in detail in chapter 1.4.

The crystal structure of the extracellular segment of integrin αvβ3 containing the integrin-ligand binding region had been also solved. It is found to be in the connecting area between the β-propeller of integrin αv- and the βA- domain of the integrin β3-head part (Xiong et al., 2002, 151-155).

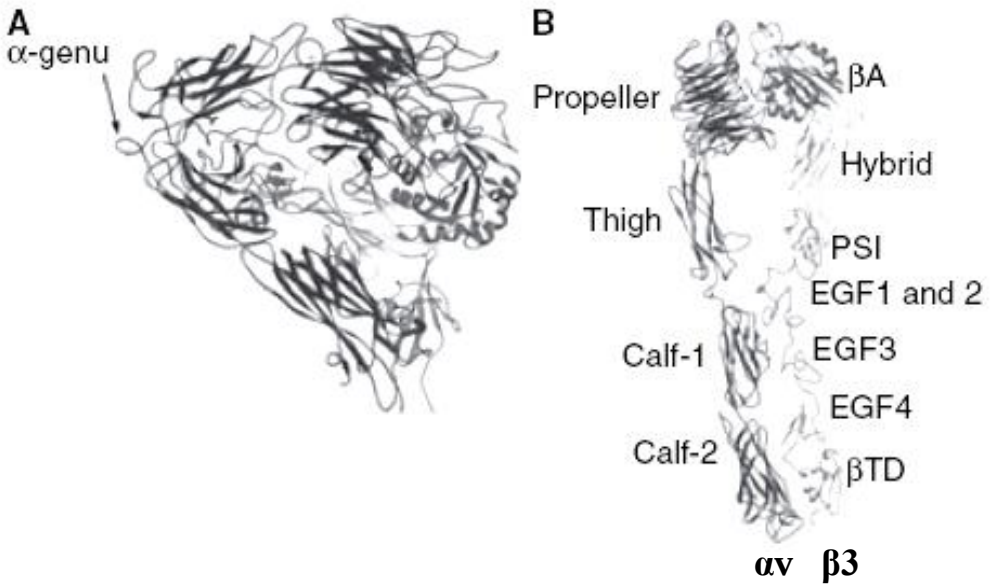

Figure 3 Structure of the extracellular segment of integrin αvβ3
(A) Figure of the bent (inactive, resting) conformation of integrin αvβ3. Represented is the *genu* domain that permits integrin α- and β-tails to form a V-shaped structure; (B) Figure of the extended integrin αv- and β3-extracellular segments (active, ligand binding state); the integrin αv extracellular portion consists of an amino-terminal β-propeller domain followed by a *thigh*- and two *calf*-domains; the integrin β3 extracellular portion consists of an amino-terminal βA-domain and Ig-like hybrid followed by PSI-domain, four tandem EGF-like repeats, and a β-tail-domain (Bennett et al., 2009, 200-205). (Figure adapted from Bennett et al., 2009, 200-205).

The extra- and intracellular domains of the integrin αv- and β3-subunit, respectively, are linked by a single TMD. Less is known about the α/β-TMD, however, it seems to be an important structure for signal transduction across the cell membrane and plays a key role in the activation of the integrin receptor (Li et al., 2004, 26666-26673, Arndt, 2005, 93-141). The TMD of the integrin αv- and β3-chain is 23 amino acids long and share specific conserved interacting regions (Figure 4). There is evidence that those interacting regions for both integrin TMD are represented by the conserved motif, the GxxxG-like motif, which is similar to the GxxxG-motif of the well-characterized homodimeric erythrocyte protein glycophorin A (GpA) (Lemmon et al., 1992, 7683-7689, Senes et al., 2004, 465-479). Knowing that the GpA GxxxG-motif is important for mediating the strong interaction of GpA-TMD helices, Senes and co-workers investigated the involvement of GxxxG-like motif in a variety of other proteins, including signal transduction proteins, such as integrins (Senes et al., 2004, 465-479). The authors found out that integrin-TMD contain a GxxxG-like motif which might control the heterodimeric and interconnection between the TMD of both integrin chains. TMD thus appears to be important structures

for integrin activation (Li et al., 2001, 12462-12467, Li et al., 2004, 26666-26673, Schneider and Engelman, 2004, 9840-9846, Gottschalk, 2005, 703-712, Gahmberg et al., 2009, 431-444).

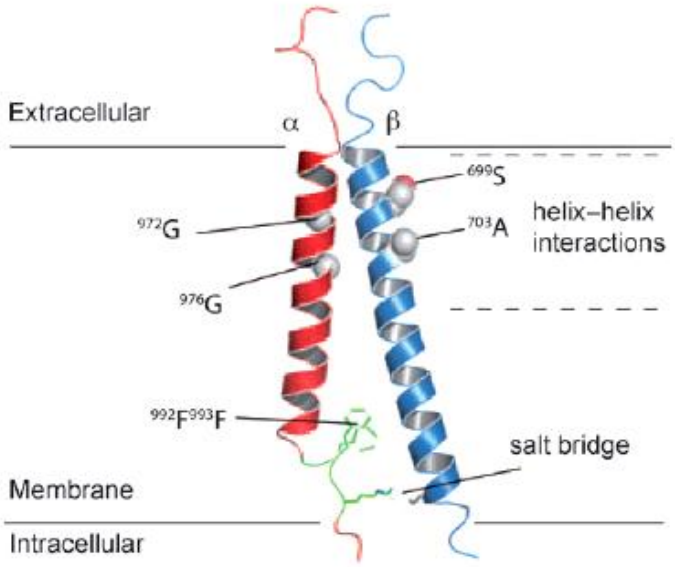

Figure 4 Scheme of the integrin α/β TMD
The integrin α-subunit is shown in red and the integrin β-subunit in blue. Two different interactions regions of the α-subunit are represented, one proximal to the membrane intracellular face comprising the conserved GFFKR (^{992}F^{993}F) motif (green) and the other near the extracellular domain comprising the conserved ^{972}Gxxx^{976}G motif (gray) (x is a non-conserved amino acid). Similar motif (^{699}Sxxx^{703}A) of the β-chain is represented near the extracellular region. The intracellular contact of both integrin chains is formed by a salt bridge between the conserved R995 of α-tail and D723 of β-tail (given is an example of integrin αIIbβ3, knowing that the homology between integrin αIIbβ3 and αvβ3 is very high), (Hoefling et al., 2009, 6590-6593). (Figure adapted from Hoefling et al., 2009, 6590-6593)

The cytoplasmic domains of both, integrin αv- and β3-subunits, respectively, are relatively short (32 and 47 amino acid residues, respectively). Studies from Hughes and co-workers revealed that the cytoplasmic domains of the integrin α- and β-subunits share a similar membrane proximal organisation with apolar and polar sequences (Hughes et al., 1996, 6571-6574). Those cytoplasmic membrane-proximal parts contain motifs that are well conserved: a GFFKR motif for the cytoplasmic integrin α-tail and a LLxxxHDRE motif for the integrin β-cytoplasmic region (Calderwood, 2004, 657-666). In this membrane proximal part, an electrostatic contact is proposed via a putative salt bridge between the conserved R995 of the integrin α-cytoplasmic tail and D723 of the

cytoplasmic domain of the integrin β-tail (Figure 4 and Figure 5). Many studies provide evidence that this electrostatic interface is also an important player during conformational changes occurring in integrin activation (Hughes et al., 1996, 6571-6574, Travis et al., 2003, 192-197, Imai et al., 2008, 5007-5015, Lau et al., 2009, 1351-1361, Yang et al., 2009, 17729-17734).

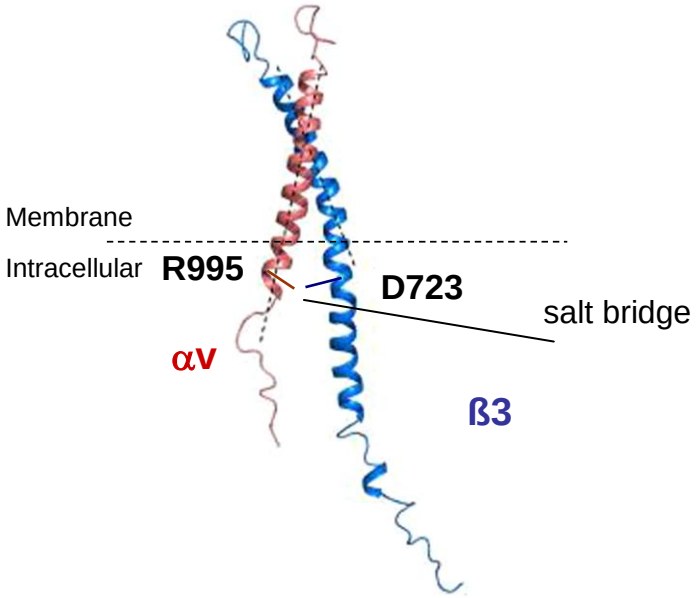

Figure 5 Scheme of the integrin αvβ3 cytoplasmic tail
An intracellular electrostatic interaction between the integrin αv- and β3-subunits is formed by a salt bridge established between the conserved R995 of the integrin αv-tail and D723 of the integrin β3-tail (given is an example of integrin αIIbβ3, knowing that the homology between integrin αIIbβ3 and αvβ3 is very high). (Figure adapted from Yang et al., 2009, 17729-17734).

1.3.2 Functions of integrin αvβ3 in angiogenesis and cancer progression

Integrin αvβ3 is an ubiquitous adhesion and signaling receptor that interacts with several ligands, such as VN, fibronectin, laminin, osteopontin, and collagen. Those ECM proteins recognise integrin αvβ3 via the tripeptide motif RGD (Arg- Gly- Asp). As a consequence of the different ligands, this integrin plays an important role in diverse biological processes such as cell migration, tumor invasion, bone resorption, angiogenesis, and immune response (Horton, 1997, 721-725, Hermann et al., 1999, 767-775, Humphries et al., 2006, 3901-3903, Harburger and Calderwood, 2009, 159-163).

The functional role of integrin αvβ3 has been extensively studied in context with osteoclastogenesis and bone resorption. Osteoclastogenesis and bone resorption plays an important part in the pathogenesis of rheumatoid arthritis (RA). Integrin αvβ3 has been found to be highly expressed on activated osteoclasts, responsible for the bone erosion and resorption during the disease of rheumatoid arthritis (Wilder, 2002, 96-99).

Of particular interest, integrin αvβ3 also plays a critical role in pathological angiogenesis and tumor progression, due to its expression on endothelial and tumor cells. High expression of integrin αvβ3 is found on activated endothelial cells involved in these pathological cell functions (Somanath et al., 2009, 177-185, Streuli and Akhtar, 2009, 491-506), whereas it is typically not expressed on quiescent endothelial cells. Integrin αvβ3 expressed in tumor cells appears to be an important marker for angiogenesis (Zhaofei Liu, 2008, 329–339).

Tumor angiogenesis depends on vascular endothelial growth factor (VEGF) stimulation and endothelial cell activation, adhesion, proliferation, and migration (Eliceiri and Cheresh, 1998, 741-750). Many studies have investigated the role of integrin αvβ3 in all of those events (Somanath et al., 2009, 177-185, Streuli and Akhtar, 2009, 491-506). In fact, it was shown that disruption of integrin αvβ3 ligation by blocking-antibodies prevents blood vessels formation in tumors without detectably influencing pre-existing blood vessels. Since integrin αvβ3 had been identified as marker for tumor vascularisation, RGD peptides and antibodies directed to integrin αvβ3 had been developed as tools for cancer imaging and targeted therapy. This anti-angiogenic therapy had been tested *in vitro* and in clinical trials *in vivo* with promising results in various malignancies, such as breast and (Harms et al., 2004, 119-128), prostate cancer (Beekman et al., 2006, 299-302), as well as glioblastoma (Desgrosellier, 2010, 9-22). In order to develop new generation of targeted therapy several studies investigated the interconnection between integrin αvβ3 expression levels and aggressiveness of tumor cells *in vitro* (Liapis et al., 1997, 443-449, Cruet-Hennequart et al., 2003, 1688-1702, Hapke et al., 2003, 1073-1083). Elevated expression level of integrin αvβ3 were found in tissue sections of invasive ovarian cancer cells compared to ovarian tumors of low malignant potential (LMP) (Liapis et al., 1997, 443-449). Cruet-Hennequart and co-workers investigated the role of integrin αvβ3 in ovarian cancer cell proliferation and invasiveness. They observed in both, the ovarian cancer cell line IGROV1 and SKOV-3, respectively, that integrin αvβ3 is an indicator of enhanced cell proliferation (Cruet-Hennequart et al., 2003, 1688-1702). Hapke and co-workers showed also increased

adhesion, migration, and proliferation in OV-MZ-6 ovarian cancer cells associated with elevated integrin αvβ3 expression levels (Hapke et al., 2003, 1073-1083).

1.3.3 Integrin αvβ3 crosstalk with the epidermal growth factor receptor

In various studies, the cooperation of integrin αvβ3 with other factors known to be involved in tumor progression had been investigated (Moro et al., 2002, 9405-9414, Hapke et al., 2003, 1073-1083, Lössner et al., 2008, 2746-2761). In that regard, studies showed that integrin αvβ3-mediated intracellular-signaling cascades lead to alterations in genes expression patterns (Kim et al., 2008, 479-483, Lössner et al., 2008, 2746-2761, Lössner et al., 2009, 367-375, Streuli and Akhtar, 2009, 491-506). One among those genes, of particular interest for the present work, is the epidermal growth factor receptor (EGF-R). It was observed that EGF-R expression correlates with that of integrin αvβ3 in ovarian cancer cells (Hapke et al., 2003, 1073-1083, Lössner et al., 2008, 2746-2761).

The EGF-R, a receptor tyrosine kinase (RTK), is important for the regulation of normal ovarian follicle development and growth of the ovarian epithelial surface (Hapke et al., 2003, 1073-1083, Lössner et al., 2008, 2746-2761). High EGF-R levels are associated with elevated cell proliferation and increased cell migration *in vitro*. EGF-R activation follows its binding to one of its multiple ligands, EGF, transforming growth factor-α, or amphiregulin. Ligand binding induces the intrinsic receptor tyrosine kinase activity and leads to cytoplasmic auto- and transphosphorylation. The EGF-R is activated and triggers downstream signaling pathways (Jorissen et al., 2003, 31-53). Disturbing the balance of this activation mechanism might be involved in the pathophysiological functions of the EGF-R.

The EGF-R is known to be overexpressed in one third of epithelial cancers, including ovarian cancer. The role of the EGF-R in the pathogenesis of ovarian cancer development is yet not fully understood. It is shown that EGF-R expression is elevated in malignant ovarian cancer cells compared to its expression level in benign tumors or normal ovary cells (Hapke et al., 2003, 1073-1083). Some recent work showed that EGF-R and integrin αvβ3 activation are interconnected, however, without fully unravelling the precise underlying mechanism (Cabodi et al., 2004, 438-442, Lössner et al., 2008, 2746-2761, Streuli and Akhtar, 2009, 491-506). Resent studies even showed that integrin αvβ3 leads to a significant upregulation of EGF-R expression and activity that is due to prominent

integrin αvβ3-mediated enhancement of EGF-R promoter activity (Cabodi et al., 2004, 438-442, Lössner et al., 2008, 2746-2761). The complex relationship between integrins and EGF-R and their cooperation in cell signaling mechanisms remain to be further elucidated. Since they are both involved in the progression of diverse human ovarian cancers, they represent targets potential for cancer therapeutical intervention.

1.4 Conformational changes during integrin activation

Integrins adopt several different conformational states during their activation. Many of these are transient. The current model for integrin activation suggests a three-state-mechanism, associated with the ligand binding affinity: low-affinity resting state, intermediate, and high-affinity activated state (Boettiger et al., 2001, 1227-1237, Gottschalk et al., 2002, 1800-1812, Takagi et al., 2002, 599-511, Luo and Springer, 2006, 579-586, Alon and Dustin, 2007, 17-27, Luo et al., 2007, 619-647, Anthis and Campbell, 2011, 191-198).

The extracellular domains of integrin α- and β-subunits have been found in two conformational states, bent and extended. The bent conformation is supposed to represent the inactive, resting state of integrins presenting a low-affinity binding to its ligand. Activation of the receptor results in leg extension and opening of the headpiece of the extracellular domains. These conformational rearrangements are essential for the activation and result in high-affinity ligand binding (Xiong et al., 2001, 339-345, Takagi et al., 2002, 599-511, Luo and Springer, 2006, 579-586, Zhu et al., 2008, 849-861).

The TMD of integrin α- and β-subunits also plays a role in signal transmission and fine-tuning of structural rearrangements involved in integrin activation (Arndt et al., 2005, 93-141). Some previous studies revealed that the integrin TMD form a right-handed coiled-coil structure in the resting state building an electrostatic interface between both chains (Gottschalk, 2005, 703-712, Yang et al., 2009, 17729-17734). This electrostatic interaction is supposed to be formed by specific regions. Senes and co-workers found out that one of those specific regions in the integrin TMD is highly similar to the GxxxG-motif within the TMD of GpA which, there, mediates strong homodimeric TMD association (Senes et al., 2004, 465-479). Further studies indicated that integrin TMD dimerization represents the resting inactive state of integrin receptors (Gottschalk et al.,

2002, 1800-1812), whereas TMD unclasping seems to be associated with integrin activation (Zhu et al., 2007, 2475-2483, Lau et al., 2009, 1351-1361).

Integrin cytoplasmic domains are short, but essential for integrin functions, since it has been demonstrated that they play a key role in integrin activation and signal transmission across the cell membrane (Travis et al., 2003, 192-197). Molecular studies revealed that integrin α- and β-subunits share a similar membrane-proximal electrostatic interaction formed by a putative salt bridge in their cytoplasmic domains (Hughes et al., 1996, 6571-6574). It is supposed that this cytoplasmic interaction stabilises the integrin receptor in the resting non-activated state. Conversely, separation of this interface might activate integrins resulting in conformational rearrangements of the extracellular domain (Hughes et al., 1996, 6571-6574, Vinogradova et al., 2002, 587-597, Kim et al., 2003, 1720-1725, Lau et al., 2009, 1351-1361). However, the connection between conformational changes of integrin cytoplasmic tail to their own extracellular region is not yet entirely understood and the functional role of a putative salt bridge implicated therein is controversially discussed. On one hand, formation of a salt bridge appears to be important for integrin activation (Hughes et al., 1996, 6571-6574, Partridge et al., 2005, 7294-7300, Imai et al., 2008, 5007-5015). On the other hand, conflicting results regarding the role of the cytoplasmic salt bridge for integrin activation have been reported by Czuchra and co-workers (Czuchra et al., 2006, 889-899). They investigated the role of salt bridge formation *in vivo* using transgenic mice which carry a point mutation of the salt bridge forming amino acid residue in the integrin β1-chain (D759A). Since no obvious phenotype was noticeable, the authors concluded that the salt bridge might not be essential for integrin activation (Czuchra et al., 2006, 889-899).

Taken together conformational changes during integrin activation imply complex molecular and dynamic mechanisms, including the connection of each integrin domain, i.e. extracellular, TMD and cytoplasmic. How integrin subunits associate/dissociate during activation and thereby permit signal transmission, i.e. “inside-out” and “outside-in” across the cell membrane remains still a matter of debate.

In that regard, the aim of this work is to investigate the impact of integrin TMD conformation and cytoplasmic salt bridge formation on the integrin activation.

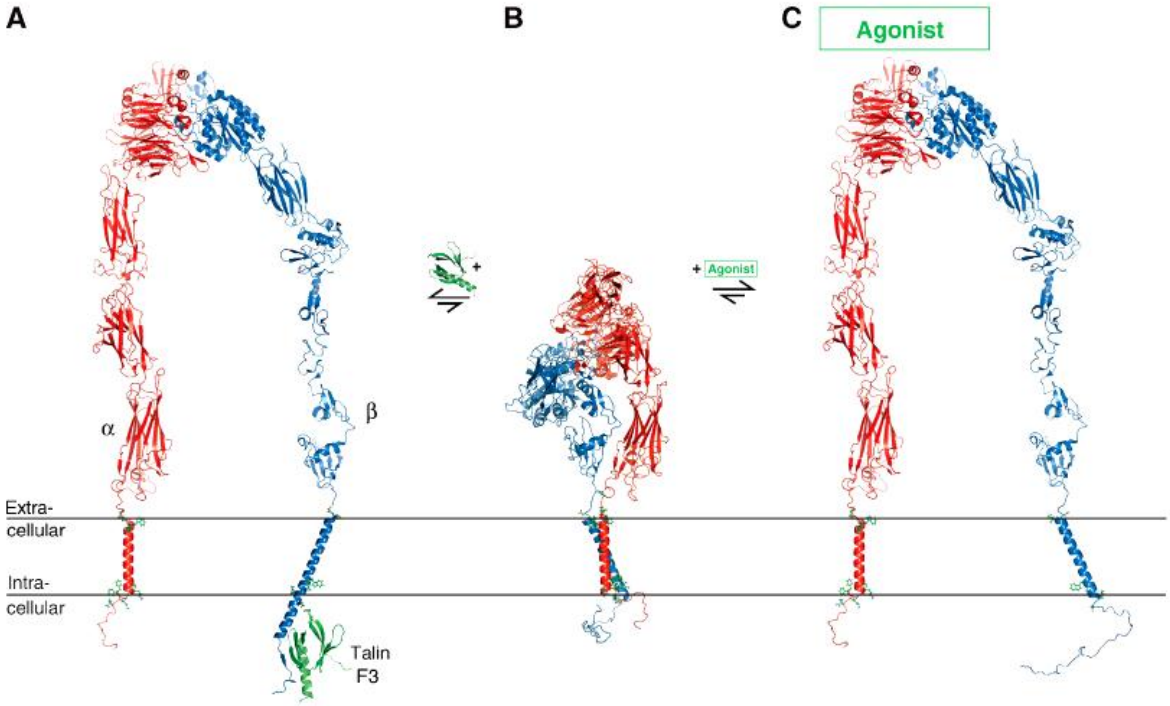

Figure 6 Illustration of integrin functional states
A) Activated integrin receptor state: inside-out activation is associated with binding of intracellular ligands, such as talin to the cytoplasmic integrin β-domain followed by dissociation of the TMD structure and activation of the extracellular domain with legs extension and exposition of the extracellular headpiece (Takagi et al., 2002, 599-511, Calderwood, 2004, 657-666, Gahmberg et al., 2009, 431-444). B) Resting state: closed conformation of the integrins represents a compact structure with the extracellular integrin α- and β-subunits bent or folded back onto the membrane proximal domains (Xiong et al., 2002, 151-155, Adair et al., 2005, 1109-1118, Zhu et al., 2008, 849-861), additionally stabilised by electrostatic interactions in the TMD (Gottschalk et al., 2002, 1800-1812, Partridge et al., 2005, 7294-7300) and the membrane proximal cytoplasmic tail region (Hughes et al., 1996, 6571-6574, Vinogradova et al., 2002, 587-597). C) Activated integrin receptor: outside-in activation associated with binding of extracellular ligands to the exposed extracellular headpiece and extended tailpieces fused to α- and β-TMD structures and connected to the respective cytoplasmic domain (Figure adapted from Lau et al., 2009, 1351-1361).

1.5 Aim of the work

Three integrin conformational states are proposed so far: resting, intermediate, and activated states (Boettiger et al., 2001, 1227-1237, Gottschalk et al., 2002, 1800-1812, Luo and Springer, 2006, 579-586, Alon and Dustin, 2007, 17-27, Luo et al., 2007, 619-647, Anthis and Campbell, 2011, 191-198). The molecular mechanism implicated in changing from one conformational state to another is very complex and still a matter of scientific debate. TMD and cytoplasmic conformational changes are known to be involved in integrin activation.

The aim of the present study was to generate integrin αvβ3 mutants of the transmembrane and cytoplasmic domain which allow the analysis of the effects of cytoplasmic and transmembrane conformations on integrin activation.

First, we created mutants of the integrin αvβ3 cytoplasmic salt bridge. For this, we exchanged the salt bridge-forming amino acids (αv_{R995D}; $\beta 3_{D723R}$) in the individual integrin chains. To analyse the effect of such mutants on integrin activation, OV-MZ-6 cells were stably transfected with different combinations of integrin αv- and β3-chains to express αvβ3 integrin variants of forming a putative salt bridge (αvβ3 WT or a charge reversal mutant $\alpha v_{R995D}\beta 3_{D723R}$) or wherein this salt bridge has been disrupted ($\alpha v_{R995D}\beta 3$ or $\alpha v\beta 3_{D723R}$).

Second, we created mutants the integrin αvβ3 TMD domain, i.e. TMD-GpA and TMD-GpA-I. The complete integrin αv-TMD WT and integrin β3-TMD WT were exchanged by the TMD-GpA motif. TMD-GpA served as a model of strong TMD dimerization. As a control, we generated TMD-GpA-I construct knowing to no longer support the TMD association (Lemmon et al., 1992, 7683-7689). The central motif of the TMD-GpA (GxxxG) were changed to TMD-GpA-I (GxxxI). The latter serves as a dissociated TMD model. After stable tansfection in OV-MZ-6 ovarian cancer cells the effect of the two chimeras were studied:

i) on human ovarian cancer cell proliferation
ii) on the EGF-R expression
iii) interaction between integrin αvβ3 TMD mutants and EGF

2 Materials and methods

2.1 Materials

2.1.1 Cell line

The human ovarian cancer cell line OV-MZ-6 had been previously established by isolating ovarian cancer cells from malignant ascites of a patient afflicted with an advanced ovarian cystadenocarcinoma (Möbus et al., 1992, 76-84).

2.1.2 Bacterial strain

Escherichia coli bacterial strain used for replication of plasmid DNA.

XL1- Blue supercompetent cells	Stratagene, La Jolla, CA, USA

2.1.3 Cell culture reagents

DMEM + GlutaMAX™-I (Dulbecco`s modified eagle medium with Glutamax I)	Invitrogen Life Technology, Carlsbad, CA, USA
Dulbecco`s phosphate buffered saline (DPBS)	Invitrogen Life Technology
Fetal calf serum (FCS)	Invitrogen Life Technology
4-(2-hydroxyethyl)-1-piperazineethanesulfonic acid (HEPES)	Invitrogen Life Technology
L-arginine and L-asparagine	Sigma-Aldrich GmbH, Steinheim, Germany
Ethylene diamine tetraacetic acid (EDTA) 1% (w/v)	Biochrom AG, Berlin, Germany
Human epidermal growth factor, recombinant, expressed in *Escherichia coli*	Sigma-Aldrich, Saint Louis, USA

2.1.4 General chemicals

3-(4,5-dimethylthiazoyl-2-yl)-2,5-diphenyl tetrazolium bromide (MTT)	Sigma-Aldrich GmbH
Paraformaldehyde (PFA)	SERVA Electrophoresis GmbH, Heidelberg, Germany
Bovine serum albumin (BSA)	Sigma-Aldrich GmbH

Dimethyl sulfoxide (DMSO)	Sigma-Aldrich GmbH
Deoxyribonucleotide (dNTP)	Peqlab, Erlangen, Germany
Isopropanol	Sigma-Aldrich GmbH
Ethanol 70%	Sigma-Aldrich GmbH
1kb DNA ladder peqGOLD	Peqlab
Ethidium bromide solution 1% (w/v)	Carl Roth GmbH, Karlsruhe, Germany
Trypan blue solution 0.4% (w/v)	Sigma-Aldrich GmbH
Bacto™ agar	Becton Dickinson BD Heidelberg, Germany
Glycerol	CarlRoth GmbH

2.1.5 General solutions and buffers

SOLUTION/BUFFER	CONCENTRATION	INGREDIENTS
DNA loading buffer for agarose gel electrophoresis	0.025 g 0.025 g 3.0 ml ad 10 ml	xylene cyanol bromophenol blue glycerol ddH_2O
Tris-acetate-EDTA (TAE) for agarose gel	2.0 M 0.5 M 2 mM pH 7.9	tris/HCL Na-acetate EDTA
Phosphate buffered saline (PBS)	137 mM 2.7 mM 7.3 mM 1.47 mM	NaCl KCl Na_2HPO_4 KH_2PO_4
PCR-buffer (10x)	100 mM 100 mM 200 mM 20 mM 1 % (v/v) 1 mg/ml	KCl $(NH_4)_2SO_4$ tris-HCl (pH 8.8) $MgSO_4$ triton X-100® nuclease-free bovine serum albumin (BSA)
Tris-EDTA (TE) buffer	10 mM 1 mM	tris-HCl (pH 7.5) EDTA
Lysogeny broth (LB) medium (liquid) for bacterial cultures	1 % (w/v) 0.5 % (w/v) 0.5 % (w/v)	bacto-tryptone yeast extract NaCl ddH_2O adjust pH to 7.0 with NaOH

SOLUTION/BUFFER	CONCENTRATION	INGREDIENTS
LB medium (fast)	1.5 % (w/v)	bacto-agar ad to LB Media liquid
Resuspension buffer S1 for isolation of plasmid DNA	50 mM 10 mM 100 µg/ml pH 8.0	tris/HCL EDTA RNase A
Lysis buffer S2 for isolation of plasmid DNA	200 mM 1 % (w/v)	NaOH sodium dodectyl sulfate
Neutralisation buffer S3 for isolation of plasmid DNA	2.8 M pH 5.5	potassium acetate
Equilibration buffer N2 for isolation of plasmid DNA “maxiprep”	100 mM 15 % (v/v) 900 mM 0.15 % (v/v) pH 6.3	tris ethanol KCl triton X-100 adjusted with H_3PO_4
Wash buffer N3 for isolation of plasmid DNA “maxiprep”	100 mM 15 % (v/v) 1.15 M pH 6.3	tris ethanol KCl adjusted with H_3PO_4
Elution buffer N5 for isolation of plasmid DNA “maxiprep”	100 mM 15 % (v/v) 1 M pH 8.5	tris ethanol KCl adjusted with H_3PO_4
Solution A for FACS analysis	0.1 M	Na_2HPO_4 ddH_2O
Solution B for FACS analysis	0.1 M	Na_2HPO_4 ddH_2O
PFA fixans	4 % (w/v)	paraformaldehyde A+B solution
NEBuffer 1 Kpn I enzyme buffer	10 mM 10 mM 1 mM pH 7.0	bis-tris-propane-HCl $MgCl_2$ dithiothreitol
NEBuffer 2 Hind III enzyme buffer	10 mM 50 mM 10 mM 1 mM pH 7.9	tris-HCl NaCl $MgCl_2$ dithiothreitol
NEBuffer 3 Eco RV, Bcl I, enzyme buffer	50 mM 100 mM 10 mM 1 mM pH 7.9	tris-HCl NaCl $MgCl_2$ dithiothreitol

SOLUTION/BUFFER	CONCENTRATION	INGREDIENTS
NEBuffer 4 Xba I, Dpn I, enzyme buffer	20 mM 50 mM 10 mM 1 mM pH 7.9	tris-acetate potassium acetate magnesium acetate dithiothreitol
NEBuffer Eco RI enzyme buffer	100 mM 50 mM 10 mM 0.025 % (v/v) pH 7.5	tris-HCl NaCl $MgCl_2$ triton X-100

2.1.6 Expression plasmid

pcDNA™ 3.1/myc-His	Invitrogen Life Technology (Figure 7)

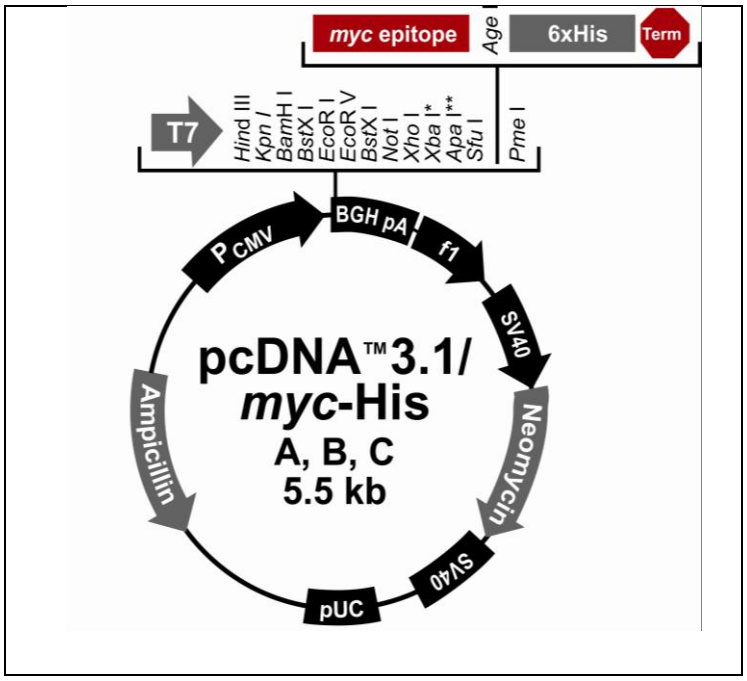

Figure 7 pcDNA™ 3.1/myc-His vector
The pcDNA3.1 myc His B vector contains the ampicillin resistance gene used for selection of transformed *E. coli*. Neomycin resistance gene was used for the selection of stably transfected cell clones.

2.1.7 Antibiotics

ANTIBIOTICS	CONCENTRATION	ORIGIN
Geneticin® G 418 sulfate	1 g/l	Invitrogen Life Technology
Ampicillin	100 µg/ml	Sigma-Aldrich GmbH

2.1.8 Enzymes

ENDONUCLEASES	ENZYME BUFFER	ORIGIN
Eco RI	NEBuffer Eco RI	BioLabs®Inc. Frankfurt am Main, Deutschland
Eco RV	NEBuffer 3	BioLabs®Inc.
Bcl I	NEBuffer 3	BioLabs®Inc.
Dpn I	NEBuffer 4	BioLabs®Inc.
Kpn I	NEBuffer 1	BioLabs®Inc.
Hind III	NEBuffer 2	BioLabs®Inc.
Xba I	NEBuffer 4	BioLabs®Inc.

OTHER ENZYMES	SPECIFICS	ORIGIN
PfuTurbo® DNA polymerase (2.5 U/µl)	no proofreading function thermostable	Stratagene
TAQ DNA polymerase	no proofreading function thermostable	Stratagene

2.1.9 Kits

QuikChange® site-directed mutagenesis kit	Stratagene
NucleoSpin™-kit for plasmid DNA purification	Macherey-Nagel, Easton, PA, USA
NucleoBond™-kit for plasmid DNA purification mini/midi/maxi	Macherey-Nagel

2.1.10 Primers for *in vitro* site-directed mutagenesis

Two oligodeoxynucleotide primers (s:sense and as:antisense) with the desired mutation (underlined amino acids) are used for the amplification of the pcDNA3.1 myc His B vector encompassing the integrin β3 cDNA-insert.

a) Salt bridge oligodeoxynucleotide primers

β3-salt s:

5´-CCTCATCACCATCCACCGCCGAAAAGAGTTCGCTAAATTTGAGG-3´

β3-salt as:

5´-CCTCAAATTTAGCGAACTCTTTTCGGCGGTGGATGGTGATGAGG-3´

b) TMD oligodeoxynucleotide primers

β3-TMD 1.mut s:

5´-CCTGACATCCTGGTGATCATCTTCGCAGTGATGGGGGCC-3´

β3-TMD 1.mut as:

5´-GGCCCCCATCACTGCGAAGATGATCACCAGGATGTCAGG-3´

β3-TMD 2. mut s:

5´-GGTGATCATCTTCGGAGTGATGGCGGGCGTTCTGCTCATTGG-3´

β3-TMD 2.mut as:

5´-CCAATGAGCAGAACGCCCGCCATCACTCCGAAGATGATCACC-3´

β3-TMD 3.mut s:

5´-GGAGTGATGGCGGGCGTTATCGGCACTATCCTTCTCGCCCTGCTCATCTGG-3´

β3-TMD 3.mut as:

5´-CCAGATGAGCAGGGCGAGAAGGATAGTGCCGATAACGCCCGCCATCACTCC-3´

β3-TMD 4.mut s:

5´-CCCTGACATCACGCTGATCATCTTCGGAGTGATGG-3´

β3-TMD 4.mut as:

5´-CCATCACTCCGAAGATGATCAGCGTGATGTCAGGG-3´

β3-TM-ile s:

5´-GCTGATCATCTTCGGAGTGATGGCGATCGTTATCGGC-3´

β3-TM-ile as:

5´-GCCGATAACGATCGCCATCACTCCGAAGATGATCAGC-3´

2.1.11 Antibodies

ANTIBODIES	CONCENTRATION	ORIGIN
Monoclonal mouse IgG (mAb) directed against EGF-R	100 µg/ml	Stressgen, Victoria, Canada
mAb-directed against p-EGF-R	250 µg/ml	Becton-Dickinson
Polyclonal goat-anti-mouse IgG, Alexa-488 conjugated	1.2 mg/ml	Invitrogen

2.1.12 Instruments

Perkin-Elmer thermocycler 2400	Perkin ELMER, Norwalk, California, USA
Agarose gel electrophoresis system	Biometra, Goettingen, Germany
Serva blue power system	Serva, Heidelberg, Germany
Eppendorf thermomixer 5436	Eppendorf, Hamburg, Germany
Eppendorf centrifuge 5417C	Eppendorf
Heraeus labofuge 400R function line	Kendro, Osterode, Germany
centrifuge Avanti™ 30	Beckman, München, Germany
Heraeus function line BB16 cell incubator	Heraeus, Hanau, Germany
Eppendorf bio photometer	Eppendorf
ELISA reader spectra II	STL Labinstruments, Crailsheim, Germany
FACScalibur flow cytometer	Becton-Dickinson
microscope Axiovert 25	Zeiss, Jena, Erlbach, Germany
Bacterial incubator	Edmund Buehler, Hechingen, Germany
SpeedVac SVC 100	Savant, Wertheim, Germany
Labor-pH-meter CG 842	Schott, Meinz, Germany
Neubauer hemocytometer	Paul Marienfeld GMBH & CO KG, Lauda-Koenigshofen, Germany

2.2 Methods

2.2.1 Cell culture

a) Medium composition for cell culture

Complete medium for OV-MZ-6 cells:

- DMEM with GlutaMAX™-I
- 10 mM HEPES
- 550 mM arginine
- 272 mM asparagine
- 10 % (v/v) FCS

Selection medium for stably transfected OV-MZ-6 cells:

- Complete medium supplemented with G 418 at a final concentration of 1g/l

b) Splitting of cells

The human ovarian cancer cell line OV-MZ-6 was cultured for 3 or 4 days in complete DMEM at 37°C/ 5% (v/v) CO_2 in a Heraeus function line BB16 cell incubator (see 2.1.12) till cell monolayers reached a confluency of approximately 60 to 80%. Then, cells were washed once in sterile PBS, and incubated in PBS, 0.02% (w/v) EDTA at 37°C for about 3 to 5 min. When cells started to round up, they were detached and centrifuged at 1,500 x g for 3 min. Cell pellets were resuspended in fresh medium and passed in a new cell culture flask.

c) Cryoconservation of cells

5 x 10^6 cells were detached from the cell culture flasks as described, centrifuged, and resuspended in freezing-medium (90% (v/v) FCS; 10% (v/v) DMSO). Cell suspensions were immediately stored on ice. After a cool down-step at -80°C overnight, cells were transferred to liquid nitrogen (-196°C) for long-time storage.

2.2.2 *In vitro* site-directed mutagenesis

a) Primer design guidelines

According to the guidelines, the oligodeoxynucleotide primer were designed such that the mutated bases were in the middle of the primers and the CG content was about 40%. Care was also taken that the 3´- and 5´-terminal bases of the primers contained one or more C or G bases. Primer length ranged between 25 and 45 bases; with a melting temperature (Tm) ≥ 78°C. The melting temperatures were calculated with the following formula:

$$Tm=81.5 + 0.41(\%\ GC) - 675/N - \%\ mismatch$$

- N is the primer length in bases
- Values for % GC and % mismatch are whole numbers

b) Polymerase chain reaction buffer

PCR amplification was performed in a reaction medium containing:

- 10 ng DNA plasmid (see 2.1.6)
- 20 pmol oligodeoxynucleotide reverse primer
- 20 pmol oligodeoxynucleotide forward primer
- 2.5 mM dNTP mix (see 2.1.4)
- 10x PCR-Buffer (5 µl)
- ad double-distilled water (ddH_2O) to a final volume of 50 µl

Finally, 1 µl of PfuTurbo® DNA polymerase (2.5 U/µl) was added just before starting the PCR reaction.

c) Dpn I digestion of plasmid DNA

Dpn I restriction enzyme is used for digestion of the non-mutated methylated parental DNA template. The parental DNA is dam methylated and therefore sensitive to Dpn I digestion.

Medium composition for Dpn I digestion:

- 40 µl PCR product
- 5 U Dpn I
- 5 µl 10 x Dpn I enzyme buffer NEBuffer 4 (see 2.1.5)
- 4.5 µl dd H_2O

The reaction mix was incubated for 105 min at 37°C.

d) Transformation of *E.coli* bacteria with plasmid DNA

About 0.5-10 µl of Dpn I digested plasmid DNA were added to 100 µl XL1 blue supercompetent cells (see 2.1.2) and incubated for 20 min on ice. After a short heat shock for 45 sec at 42°C, the bacteria were again incubated on ice for 2 min. Then 1 ml of LB medium was added to the bacteria suspension and incubated for 1 h at 37°C. The suspension was centrifuged at 2,700 x g for 3 min to harvest the bacteria. The bacteria were resuspended in 100 µl LB medium and spread on LB-ampicillin agar plates. The plates were incubated at 37°C overnight. Colonies of *E.coli*, which had been successfully transformed and thus acquired resistance to antibiotics were picked from the agar plates. The bacteria were added to 1 ml ampicillin-LB medium and incubated overnight at 37°C under instant shaking.

For small scale plasmid analysis, a large number of colony were picked from the agar plates and each added to 1 ml of LB+ampicillin medium. "Miniprep" isolation of plasmid DNA was performed on 900 µl of the 1 ml culture in LB+ampicillin medium. The 100 µl remaining were kept for eventual further large scale plasmid amplification.

For large scale plasmid preparation the remaining 100 µl of bacterial suspension were added to 100 ml of LB+ampicillin medium.

2.2.3 Amplification, purification, and analysis of plasmid DNA

a) Small scale isolation of plasmid DNA ("miniprep")

To that aim, bacterial suspensions were harvested from LB medium by centrifugation at 2,700 x g for 5 min. Bacteria were carefully resuspended in 200 µl of chilled buffer S1 (buffer composition see 2.1.5) containing RNase A. After addition of 200 µl S2 buffer (see 2.1.5), tubes were flipped over 4 to 6 times and incubated for 2-3 min at room temperature (RT). Then 200 µl of chilled S3 buffer (see 2.1.5) were added and the bacterial suspensions mixed carefully by flipping over the tube 8 times. After incubation for 20 min on ice, a new centrifugation step was performed (17,900 x g, 5 min, 4°C). The clear supernatant was transferred into a new 1.5 ml tube and 400 µl of isopropanol added. The mixture was then centrifuged (17,900 x g, 15 min, 4°C). After careful removal of the supernatant, the DNA pellets were washed two times in 400 µl of 70% (v/v) ethanol. After a final centrifugation step, the DNA pellet was dried in the vacuum chamber SpeedVac SVC 100 (see 2.1.12). Then the DNA pellet was dissolved in 20 µl of distilled H_2O for further use.

b) Large scale isolation of plasmid DNA ("maxiprep")

The large scale isolation of plasmid DNA was done using the NucleoBond™ Plasmid Kit from Macherey-Nagel. The preparation was performed following the manufacture's instructions.

Bacterial suspensions were harvested from the LB medium by centrifugation (6,000 x g, 15 min, 4°C). Bacteria were resuspended in 12 ml of chilled buffer S1 (buffer composition see 2.1.5) containing RNase. Then, 12 ml of S2 buffer were added and suspensions flipped over 6 to 8 times. After a short incubation period of 2 to 3 min at RT, 12 ml of chilled S3 buffer were added. Then the bacterial suspensions were mixed by inverting the flasks 6 to 8 times and incubated for 5 min on ice. Meanwhile, NucleoBond® Maxi column were equilibrated with 6 ml of N2 buffer. After 5 min of incubation, a new centrifugation step (12,000 x g, 40 min, 4°C) was performed. The supernatant was past through a paper filter of the equilibrated NucleoBond® Maxi column. Then the same filter was washed two times in 32 ml of N3 buffer. After 15 ml of N5 buffer were passed

through the filter, the filter was removed. Opaque DNA pellet in 11 ml of isopropanol were two times flipped over. The mixture was then centrifuged (15,000 x g, 30 min, 4°C) and the isopropanol carefully removed. The opaque DNA pellet was washed two times in 1000 µl of 70% (v/v) ethanol. After a final centrifugation step (15,000 x g, 10 min, 4°C), ethanol was carefully removed and the DNA pellet dried for 2 min in the vacuum chamber SpeedVac SVC 100 (see 2.1.12). The DNA pellet was dissolved in 40 µl of distilled H_2O for further use.

c) Determination of DNA concentration

Concentration and purity of DNA solutions were determined by measuring the absorbance of DNA samples resuspended in H_2O at 260 nm and 280 nm, respectively. Measurement at 280 nm allowed the detection of protein impurities within the DNA samples. The measurement of the optical density (OD) at 260 nm gives a direct estimate of the concentration of double stranded DNA. The value of OD_{260} equal to 1 is known to correspond to 50 µg/ml of ds DNA. The ratio of OD_{260}/OD_{280} gives an estimate of the DNA purity. For a ratio comprised between 1.8 and 2.0 the DNA sample is considered as sufficiently pure.

d) DNA digestion by restriction endonucleases

In order to control that the plasmid DNA contained the correct DNA insert, plasmid DNA was subjected to an analytical restriction enzyme digestion. Restriction enzyme digestion was performed on 1-1.5 µg of purified plasmid DNA following the procedure as described herein above (see 2.2.3 a, b). The restriction mixture contained:

- 1 µg of purified plasmid DNA
- 1 Units of restriction enzyme
- suitable enzyme buffer for the restriction endonuclease used
- distilled H_2O up to a final volume of 20 µl

The solution was incubated for 1 h at 37°C.

e) Agarose gel electrophoresis

Analytical agarose gel electrophoresis was performed by migration of DNA in 1% (w/v) agarose gel prepared in TAE buffer (see 2.1.5), containing 0.5 µg/ml ethidium bromide for DNA staining. In order to visualize the migration front of the DNA samples and to facilitate the loading into the wells of the agarose gel, DNA was mixed with 5 x loading buffer (see 2.1.5). After carefully pipetting of the mixture into the gel pockets, an electric field of 120 V was applied to induce migration of the DNA fragments into the agarose matrices. Marker standards pecGold 1 kb DNA ladder (see 2.1.4) were used as a DNA scale ladder to determine the length of the DNA fragments. After electrophoresis, DNA was visualized under UV light due to intercalating ethidium bromide.

2.2.4 Cell proliferation assays

a) Cell counting

This method allows the determination of cell proliferation over time by counting viable cells upon trypan blue exclusion. A viable cell has an intact cell membrane which is not permeable for trypan blue. In contrast, dead cells have permeable cell membranes and thus incorporate trypan blue.

The starting cultures are performed by seeding 20,000 cells in 12-well cell culture plates in 1 ml of DMEM culture medium and incubated at 37°C/ 5% (v/v) CO_2. At distinct time points, cells were detached from the cell culture plates with PBS, 0.02% (w/v) EDTA. Cell numbers were counted after addition of 50 µl of trypan blue solution using the Neubauer hemocytometer.

b) MTT assay

This method is based on the conversion of 3-(4,5-dimethylthiazoyl-2-yl)-2,5-diphenyl tetrazolium bromide (MTT) to blue formazan product by mitochondrial dehydrogenases in vital cells. The cell number is directly proportional to this enzymatic activity.

For this assay, cells were passed to 96-well cell culture plates at a density of 10,000 cells per well. After incubation at 37°C/ 5% (v/v) CO_2 for different time periods, MTT solution

(200 µg/ml per well) was added to each well. Then cells were incubated for 4 h at 37°C/ 5% (v/v) CO_2. Thereafter, the medium was removed and 100 µl of DMSO added per well to stop the reaction and dissolve the formed formazan crystals. Cells were then incubated over night at 37°C. After that, conversion of the chromogenic substrate was recorded at 590 nm using a plate reader spectrophotometer as a measure of cell number.

c) Detection of cell proliferation upon EGF stimulation

20,000 OV-MZ-6 cells per well were passed to 12-well cell culture plates in 1 ml medium DMEM, 10% (v/v) FCS and allowed to adhere for 3 h at 37°C/ 5% (v/v) CO_2. Cells were then washed once in sterile PBS, and DMEM containing different concentration of FCS was added. After 12 h of cell cultivation, recombinant EGF (20 ng/ml) was added. As controls served cells in parallel wells which were incubated in the absence of EGF. Cell numbers were counted after distinct time intervals upon trypan blue exclusion by using the Neubauer hemocytometer.

2.2.5 Flow cytofluorometry

a) Detection of p-EGF-R expression

Cells were cultured in T75 cell culture flasks until cell monolayers reached a confluency of approximately 60 to 70%. They were then detached and counted. 100,000 cells were passed into FACS vials. To detect expression of the activated/phosphorylated EGF-R, cells were fixed with 100 µl 4% (w/v) PFA and incubated for 30 min at RT. This step allows the permeabilization of the cell membrane and the antibody to detect both intracellular as well as extracellular target molecules. After two washes in PBS, cells were blocked in 100 µl PBS, 2% (w/v) BSA for 20 min at RT. Cells were again washed two times in PBS and incubated in mAb (12.5 µg/ml) directed to the p-EGF-R for 1 h at RT. Cells were again washed in PBS and incubated in a secondary antibody, i.e. Alexa-488-conjugated goat-anti-mouse IgG (1.2 µg/ml) for 45 min at RT. After that, the cells were extensively washed in PBS and the flow cytofluorometry analysis performed by using the FACS-Calibur instrument (Becton-Dickinson).

b) Detection of EGF-R expression

The EGF-R expression was detected in fixed and also vital cells. Cell fixation was performed as outlined above. Viable cells were kept in PBS, 1% (w/v) BSA, then fixed and unfixed cells were incubated in mAB (5 µg/ml) directed to the EGF-R for 1 h at RT. Signal detection was conducted by adding secondary Alexa-488-conjugated goat-anti-mouse IgG (1.2 µg/ml) for 45 min at RT.

3 Results

3.1 Generation of integrin αvβ3 mutants

The particular aim of the present study was to generate mutants of the integrin transmembrane and cytoplasmic domain which allows the analysis of the conformational changes of transmembrane and cytoplasmic domains on integrin activation. We decided to use as a model integrin the tumor biologically relevant integrin αvβ3. We created mutant constructs of the integrin αvβ3 transmembrane and cytoplasmic domains by *in vitro* site-directed mutagenesis.

In a first approach, mutants of the salt bridge forming amino acids in the cytoplasmic domain (Figure 8) of both, the integrin αv- and β3-subunit, respectively, were generated. To that aim, a point mutation in the integrin αv- and β3-cytoplasmic domains was introduced by exchanging amino acid: αv_{R995D} and $\beta 3_{D723R}$, respectively (Figure 8). There is a good evidence that electrostatic interactions constitute a salt bridge between the cytoplasmic domains of integrin α- and β-subunits (Hughes et al., 1996, 6571-6574). This particular interaction is thought to stabilise the low affinity non-activated state. Consequently, deletion of this cytoplasmic interface has been shown to activate integrins to a high affinity state. In order to analyse the role of this membrane-proximal interface on integrin activation, cell transfectants were established either presenting this electrostatic interaction or disrupting it (see establishment of OV-MZ-6 cells paragraph 3.2).

In a second approach, both, the complete αv-TMD and β3-TMD, respectively, were exchanged by the TMD of GpA. It has been shown that integrin TMD display structural elements, highly similar to those observed for the GpA-TMD. Thus, Sens and co-workers found out that integrin TMD encompass a similar dimerization motif as the strongly associating motif GxxxG (Senes et al., 2004, 465-479). Hence, integrin αvβ3 TMD-GpA represents an integrin with a strongly dimerizing TMD. In a second construct, we generated integrin αv/β3-TMD mutants known to no longer support TMD homodimerization by inserting a point mutation in the GpA dimerization sequence GxxxG motif to obtain a GxxxI motif (Lemmon et al., 1992, 7683-7689) (Figure 8). In order to analyse the role of the conformation of the TMD sequence on integrin activation, cell transfectants were established to present clasped integrin TMD (TMD-GpA construct) or unclasped TMD association (TMD-GpA-I construct) (see establishment of OV-MZ-6 cells paragraph 3.2).

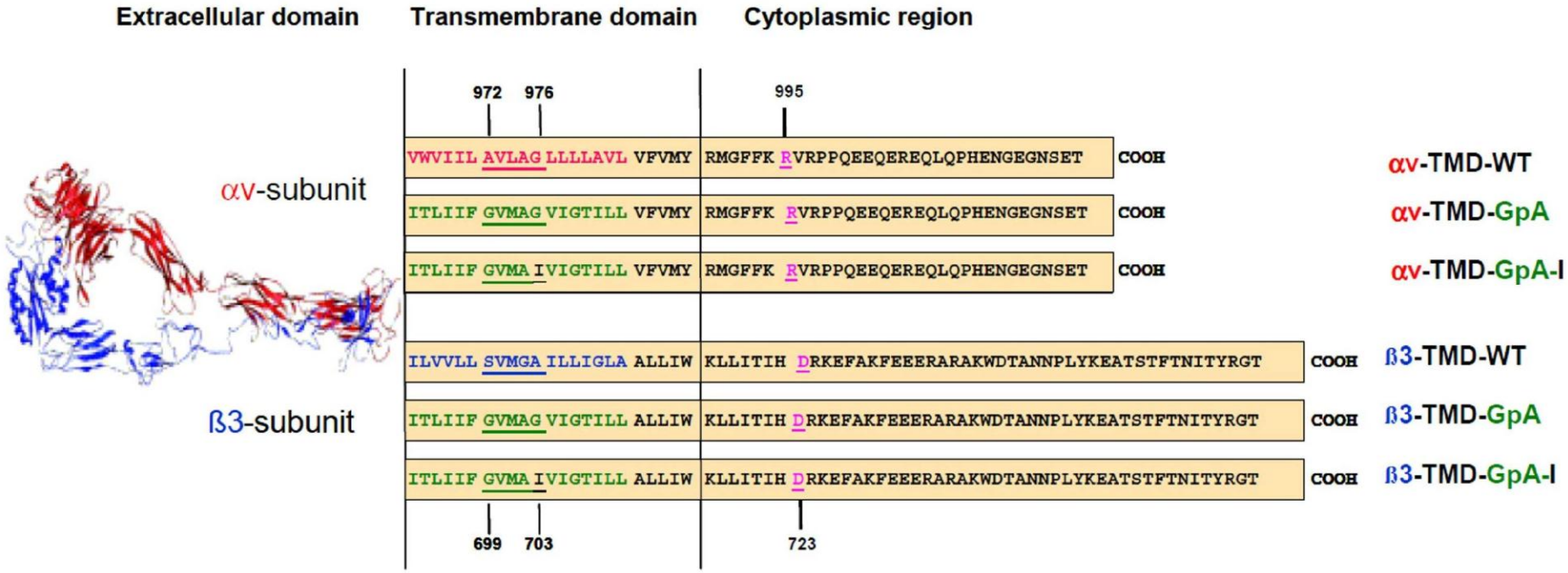

Figure 8 Design of integrin *α*vβ3-/GpA-/GpA-I-TMD constructs which were generated by *in vitro* site-directed mutagenesis.
Depicted are the sequences of the transmembrane (TMD) and cytoplasmic domains of integrin αvβ3. Integrin TMD wild type (TMD-WT) represented with the ^{972}Gxxx^{976}G-like motif in the integrin αv-subunit is underlined in red and the ^{699}Gxxx^{703}G-like motif in the β3-subunit is underlined in blue. Mutants of the integrin αvβ3-TMD (αvβ3-TMD-GpA; αvβ3-TMD-GpA-I) representing the GxxxG-like motif in both subunits are underlined in green. Point mutant of the integrin αvβ3-TMD-GpA-I representing the GxxxI motif in both subunits are underlined in black. The intracytoplasmic salt bridge forming amino acid of αv- (R995) and β3- (D723) subunit are underlined in pink. (courtesy U. Reuning)

The present dissertation concerned the mutation of the integrin β3-chain. The mutation of αv-chain was performed in parallel by Lilli Volkhardt.

3.1.1 Generation of integrin αvβ3 mutants by *in vitro* site-directed mutagenesis

In vitro site-directed mutagenesis of the integrin β3-chain was performed using the QuikChange Kit (see 2.1.9). This Kit requires four steps (Figure 10).

In the first step, the supercoiled double-stranded DNA (dsDNA) vector containing the integrin β3-insert is heat denatured. During the second step, two oligodeoxynucleotide primers containing the desired mutation are annealed to the plasmid DNA. These oligodeoxynucleotide primers, each being complementary to the opposite strand of the cDNA insert, serve as starting points for the amplification by PfuTurbo polymerase of each cDNA strand (see 2.1.8). The PfuTurbo DNA polymerase does not have a strand displacement activity therefore it replicates both plasmid strands without displacing the mutant oligodeoxynucleotide primers. Hence, nicked circular DNA plasmids are thus obtained by this method. In the third step, the non-mutated parental DNA template is subjected to digestion by Dpn I restriction enzyme. The Dpn I endonuclease (target sequence: 5´-GA/TC-3´) which is specific for methylated DNA digests the non-mutated parental DNA but preserves the mutated DNA strand. The parental DNA isolated from *E. coli* strains is dam methylated and therefore sensitive to Dpn I digestion. Finally the circular, nicked dsDNA product of the Dpn I digestion step is transformed into *E. coli* XL1-blue supercompetent cells (see 2.2.2 d).

To optimise the *in vitro* site-directed mutagenesis reaction, first the concentration of the DNA template was titrated. 50-70 ng of template DNA were used. The concentration of 50 ng turned out to be the optimal for the conducted PCR. PCR mixtures with a high GC content in the template DNA were supplemented with DMSO. DMSO has been shown to facilitate DNA strand separation, to avoid coiling and thus formation of secondary structurs of the template. BSA was used in the reaction mix as a carrier to promote the stabilisation of very small concentrations of proteins/enzymes contained in the buffer, and for example to inhibit their precipitation at the tube wall. In order to allow the perfect hybridisation for the mutagenesis oligodeoxynucleotide primers to their respective template DNA, the annealing temperatures of the PCR cycles were varied. Temperatures

between 24°C-17°C below the calculated melting temperature of the mutagenesis primers were used. It turned out that the optimum is by 24°C for the conducted PCR.

3.1.2 Generation of mutants of the integrin αvβ3 salt bridge

We generated mutants of the cytoplasmic putative αv-/β3-interchain salt bridge. For that, the amino acids implicated in the salt bridge formation were mutually exchanged (αv_{R995D}; $\beta 3_{D723R}$) (Figure 8 and Figure 9). Due to that, a charge reversal salt bridge was created ($\alpha v_{R995D}/\beta 3_{D723R}$) supposed to form this cytoplasmic interaction. The combination of mutated and non-mutated integrin αvβ3 ($\alpha v_{R995D}\beta 3$ or $\alpha v\beta 3_{D723R)}$ represented the disrupted cytoplasmic interaction.

β3 D723R:

WKLLITIH^{723}DRKEFAKFEEERARAKWDTANNPLYKEATSTFTNITYRGT

. . . . . **R** . . . . . .

αv R995D:

YRMGFFK^{995}RVRPPQEEQEREQLQPHENGEGNSET

. . . . . **D** . . . . . .

Figure 9 Design of integrin αvβ3 salt bridge mutant.
Depicted are the sequences of the integrin αv- and β3-cytoplasmic domains. The cytoplasmic salt bridge forming amino acid are mutually exchanged (αv_{R995D}; $\beta 3_{D723R}$) and are represented in red color.

To exchange the Asp (D723) into Arg (R723) from the integrin β3-chain, we mutated the following amino acids, **gac** into **cgc** within the cDNA encoding β3-chain present in the plasmid β3 pcDNA3.1 myc His B (Figure 11).

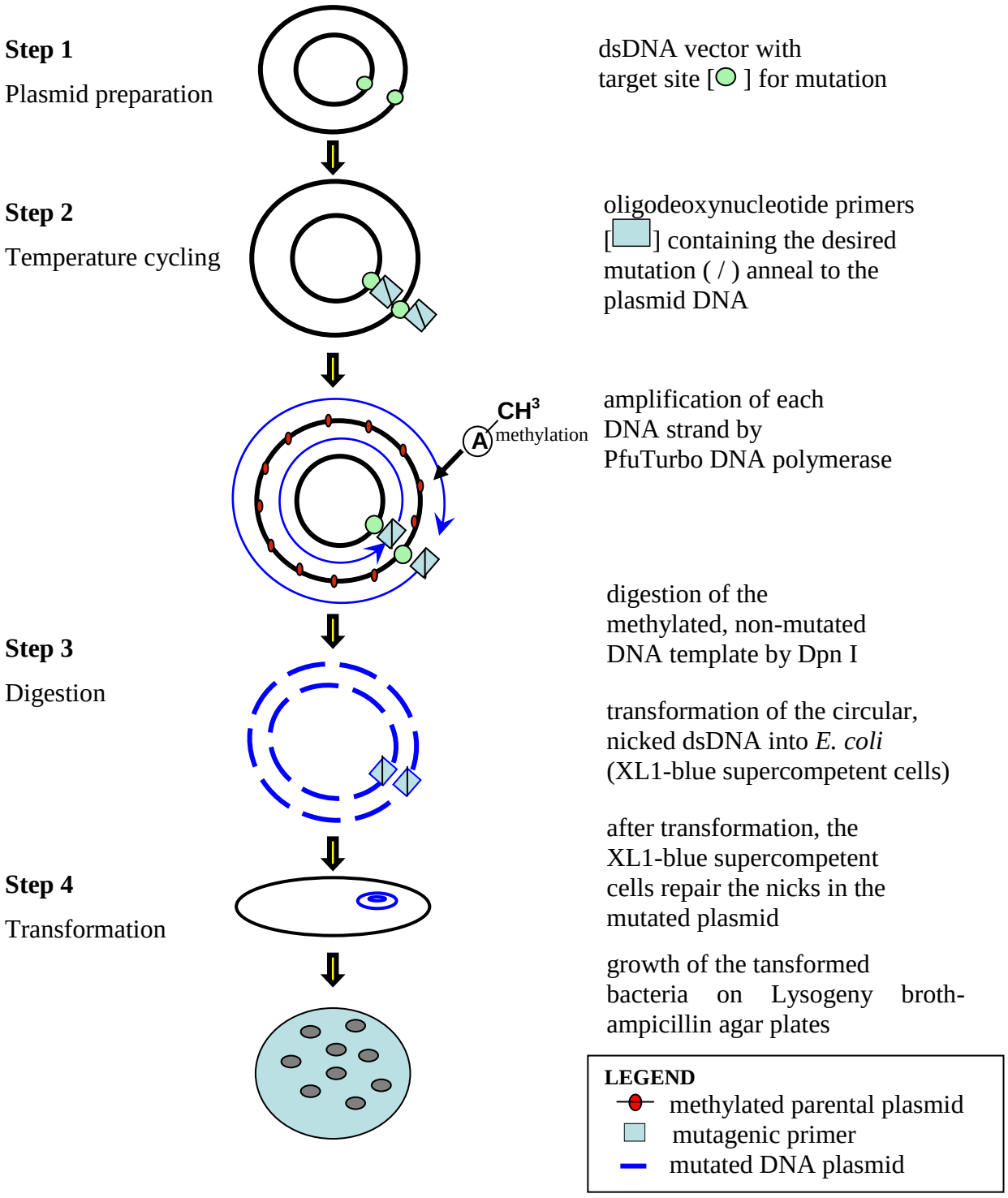

Figure 10 Scheme of the principle of the *in vitro* site-directed mutagenesis method by QuikChange.
Overview of the 4-steps procedure used by the QuikChange mutagenesis kit. In the first step, plasmid dsDNA containing the target site for mutation in the respective cDNA insert is heat denaturated. In the second step, two oligodeoxynucleotide primers containing the desired mutation are annealed to the plasmid DNA and are extended during PCR cycling by PfuTurbo polymerase. In the third step, the non-mutated methylated parental DNA template is subjected to Dpn I restriction digest. In the fourth step, the circular, nicked dsDNA product of the Dpn I digestion step is transformed into *E. coli* (XL1-blue supercompetent cells).
(based on the manual QuikChange® site-directed mutagenesis, Stratagene, 2004)

	β3 WT	β3 MUT
aa	**D (asp)**	**R (arg)**
nt	**gac**	**cgc**

Figure 11 Design of integrin β3 salt bridge mutant.
Salt bridge forming amino acid and the corresponding "codon" of integrin β3 (β3 WT) cytoplasmic domain is depicted. Point mutation of integrin β3 salt bridge (β3 MUT). (whole sequence of integrin β3 cytoplasmic domain see figure 8).
aa: amino acid
nt: nucleotide
integrin β3 amino acid and nucleotides
mutated amino acid
mutated nucleotides

In order to distinguish the mutated cDNA encoding integrin $\beta3_{D723R}$ from the cDNA encoding integrin β3 wild type, a further silent point mutation of $\beta3_{A2282G}$ was introduced within the β3 cDNA, leading to the elimination of an EcoR I restriction site (target sequence: 5´-G/AATTC-3´). The silent point mutation is 9 base pairs downstream of the mutated codon. This allowes the use of a single mutagenesis oligodeoxynucleotide primer pair. The primers were designed according to the guidelines from QuikChange Kit, Stratagene, USA (see 2.2.2 a) and were as follows:

- β3-salt forward primer:
  5´-CCTCATCACCATCCACCGCCGAAAAGAGTTCGCTAAATTTGAGG-3´
- β3-salt reverse primer:
  5´-CCTCAAATTTAGCGAACTCTTTTCGGCGGTGGATGGTGATGAGG-3´

The underlined nucleotides represent the mutated nucleotides described above.

The melting temperature of the primers was calculated according to the formula (see 2.2.2 a) to 79°C.

As template for *in vitro* site-directed mutagenesis served the expression vector pcDNA3.1 myc His B containing as insert the integrin β3 cDNA. The PCR reaction mix was prepared as described under 2.2.2 b. The PCR cycles were chosen as follows:

Step 1. initial DNA denaturation	1 min at 95°C	
Step 2. denaturation	1 min at 95°C	} 18 cycles
Step 3. annealing	1 min at 57°C	
Step 4. elongation	9 min at 68°C	
Final step	5 min at 68°C	

The PCR products were then subjected to a methylation-sensitive Dpn I restriction digest in order to destroy the methylated non-mutated template DNA strand. The PCR products

were checked by agarose gel electrophoresis and revealed one DNA fragment migration at 7.9 kb in accordance with plasmid size plus size of the β3 cDNA-insert (data not shown). *E. coli* were transformed with the PCR product after the Dpn I digestion step (see 2.2.2 d) and spread on agarose plates. 10 to 20 bacterial colonies were picked from the agar plates and the DNA isolated and analysed by restriction enzyme digestion (see 2.2.3 a). In order to prove successful mutagenesis, the plasmid DNA encompassing the β3 cDNA-insert was digested with EcoR I restriction enzyme (see 2.2.3 d). The length of the restricted DNA fragments were controlled using agarose gel electrophoresis (data not shown), knowing that EcoR I digestion of:

i) pcDNA3.1 myc His B encompassing the wild type β3 cDNA-insert give rise to three DNA fragments: 2282 bp, 5591 bp, and 7873 bp; and

ii) pcDNA3.1 myc His B encompassing the mutated β3 cDNA-insert give rise to one fragment of 7.9 kb in size.

Success of the mutagenesis was further controlled by DNA sequencing on two selected clones presenting the inserted EcoR I restriction site and resulted in confirmation of correct DNA sequence.

3.1.3 Generation of mutants of the integrin β3 transmembrane domain

3.1.3.1 Exchange of the integrin β3 transmembrane domain by that of glycophorin A

We generated integrin αv- and β3-mutants, in which the respective complete TMD of both integrin subunits were exchanged by the TMD of GpA (Figure 12). As described above (see 3.1), integrin TMD have structural elements highly similar to those observed for the GpA-TMD. GpA-TMD is shown to represent a strong TMD association mediated by the dimerization motif GxxxG. Hence, integrin TMD-GpA construct serves as a model of strong TMD dimerization resulting in a clasped integrin TMD.

β3-TMD wild type:

^{693}**ILVVLLSVMGAILLIGL**^{710}**A**

GxxxG-like motif

β3 aa	I	L	V	V	L	L	S	V	M	G	A	I	L	L	I	G	L	A
	ile	leu	val	val	leu	leu	ser	val	met	gly	ala	ile	leu	leu	ile	glu	leu	ala
β3 nt	**atc**	**ctg**	**gtg**	**gtc**	**ctg**	**ctc**	**tca**	**gtg**	**atg**	**ggg**	**gcc**	**att**	**ctg**	**ctc**	**att**	**ggc**	**ctt**	**gcc**

GpA-TMD:

^{693}**ITLIIFGVMAGVIGTIL**^{710}**L**

GxxxG-motif

GpA aa	I	T	L	I	I	F	G	V	M	A	G	V	I	G	T	I	L	L
	ile	thr	leu	ile	ile	phe	gly	val	met	ala	gly	val	ile	gly	thr	ile	leu	leu
GpA nt	**atc**	**acg**	**ctg**	**atc**	**atc**	**ttc**	**gga**	**gtg**	**atg**	**gcg**	**ggc**	**gtt**	**atc**	**ggc**	**act**	**atc**	**ctt**	**ctc**

Figure 12 Sequence of integrin β3-TMD and GpA-TMD. Overview of the amino acid sequence (red) and the corresponding codons (black) of the complete integrin β3-TMD wild type and the complete GpA-TMD. The GxxxG-like motif is represented in gray**.**
aa: amino acid
nt: nucleotide

Four successive *in vitro* site-directed mutagenesis reactions were necessary for the complete exchange of the integrin β3-TMD by that of GpA:

I. First mutation step: generation of β3-TMD mut 1

	693	694	695	696	697	698	699	700	701	702	703	704	705	706	707	708	709	710
β3 aa	I	L	V	V	L	L	S	V	M	G	A	I	L	L	I	G	L	A
	ile	leu	val	val	leu	leu	ser	val	met	gly	ala	ile	leu	leu	ile	glu	leu	ala
β3 nt	atc	ctg	gtg	gtc	ctg	ctc	tca	gtg	atg	ggg	gcc	att	ctg	ctc	att	ggc	ctt	gcc
GpA aa				I	I	F	S											
				ile	ile	phe	ser											
GpA nt				atc	atc	ttc	gca											

II. Second mutation step: generation of β3-TMD mut 2

β3 aa	I	L	V	I	I	F	S	V	M	G	A	I	L	L	I	G	L	A
	ile	leu	val	ile	ile	phe	ser	val	met	gly	ala	ile	leu	leu	ile	glu	leu	ala
β3 nt	atc	ctg	gtg	atc	atc	ttc	gca	gtg	atg	ggg	gcc	att	ctg	ctc	att	ggc	ctt	gcc
GpA aa							G			A	G	V						
							gly			ala	gly	val						
GpA nt							gga			gcg	ggc	gtt						

III. Third mutation step: generation of β3-TMD mut 3

β3 aa	I	L	V	I	I	F	G	V	M	A	G	V	L	L	I	G	L	A
	ile	leu	val	ile	ile	phe	gly	val	met	ala	gly	val	leu	leu	ile	glu	leu	ala
β3 nt	atc	ctg	gtg	atc	atc	ttc	gga	gtg	atg	gcg	ggc	gtt	ctg	ctc	att	ggc	ctt	gcc
GpA aa													I	G	T	I		L
													ile	gly	thr	ile		leu
GpA nt													atc	ggc	act	atc		ctc

IV. Fourth mutation step: generation of β3-TMD mut 4

β3 aa	I	L	V	I	I	F	G	V	M	A	G	V	I	G	T	I	L	L
	ile	leu	val	ile	ile	phe	gly	val	met	ala	gly	val	ile	gly	thr	ile	leu	leu
β3 nt	atc	ctg	gtg	atc	atc	ttc	gga	gtg	atg	gcg	ggc	gtt	atc	ggc	act	atc	ctt	ctc
GpA aa		T	L															
		thr	leu															
GpA nt		acg	ctg															

Figure 13 Stepwise design of the integrin β3-TMD mutant.
Overview of the four consecutive *in vitro* site-directed mutagenesis reactions necessary for the complete exchange of the integrin β3-TMD by that of GpA.
aa: amino acids
nt: nucleotide
integrin β3/GpA amino acid
amino acid to be mutated in the present reaction
insertion of Bcl I restriction site
mutated nucleotides
mutated amino acids

I. First mutation step: generation of integrin β3-TMD mut 1

In this first reaction, we exchanged the following amino acids: V696I; L697I; and L698F from integrin β3-TMD into GpA-TMD. In order to distinguish the mutated cDNA encoding β3-TMD mut 1 from cDNA encoding wild type β3-TMD, a Bcl I restriction site was inserted by designing respective mutagenic primers. To that aim, for exchanging V696I, the amino acid codon **gtc** was mutated into **atc**, and for exchanging L697I, the amino acid codon **ctg** was mutated into **atc**. Those mutations lead to the insertion of a Bcl I restriction site (5´-T/GATCA-3´) in the target sequence (Figure 14).

aa number	695	696	697	698	699
β3 aa	V	V	L	L	S
β3 nt	gtg	gtc	ctg	ctc	tca
GpA aa	V	I	I	F	S/G
GpA nt	gtg	atc	atc	ttc	gca

Figure 14 Design of the first integrin β3-TMD mutagenesis step.
Amino acids and the nucleotide sequences of integrin β3-TMD WT are depicted. In the first mutagenesis step amino acid V696I, L697I, and L698F from integrin β3-TMD into GpA-TMD were exchanged. To distinguish the mutated from wild type β3 TMD, the mutation was generated inserting a Bcl I restriction site.
aa: amino acid
nt: nucleotide
integrin β3-TMD amino acids and nucleotides to be mutated
GpA amino acids
nucleotides to be mutated
insertion of Bcl I restriction site

These mutations were accomplished by using the following primer pair:

- β3-TMD 1.mut forward:

  5´-CCTGACATCCTGGTGATCATCTTCGCAGTGATGGGGGCC-3´

- β3-TMD 1.mut reverse:

  5´-GGCCCCCATCACTGCGAAGATGATCACCAGGATGTCAGG-3´

The melting temperature of the primers was calculated (see 2.2.2 a) to 77°C.

As template for the first *in vitro* site-directed mutagenesis reaction served the expression vector pcDNA3.1 myc His B containing as insert the integrin β3 cDNA wild type. The PCR mixture was prepared as described (see 2.2.2 b). DMSO was added to inhibit secondary structure formation of the template DNA, especially templates with high amount of GC base pairs. DMSO is known to interfere the self-complementarity of the

DNA and to reduce the risk of interfering reactions. Two PCR mixtures were prepared containing different concentrations of DMSO, one with 8% (v/v) and one with 1% (v/v).

The PCR cycles were chosen as follows:

Step 1. initial DNA denaturation	1 min at 95°C	
Step 2. denaturation	1 min at 95°C	} 18 cycles
Step 3. annealing	1 min at 60°C	
Step 4. elongation	9 min at 68°C	
Final step	5 min at 68°C	

The parental, non-mutated methylated template DNA was digested by Dpn I restriction enzyme (see 2.2.2 c). Agarose gel electrophoresis was performed on non-digested and Dpn I-digested plasmid DNA. One DNA fragment of 7.9 kb in size represents the vector for pcDNA3.1 myc His B vector (5.5 kb) plus the integrin β3-TMD mut 1-insert (2.4 kb).

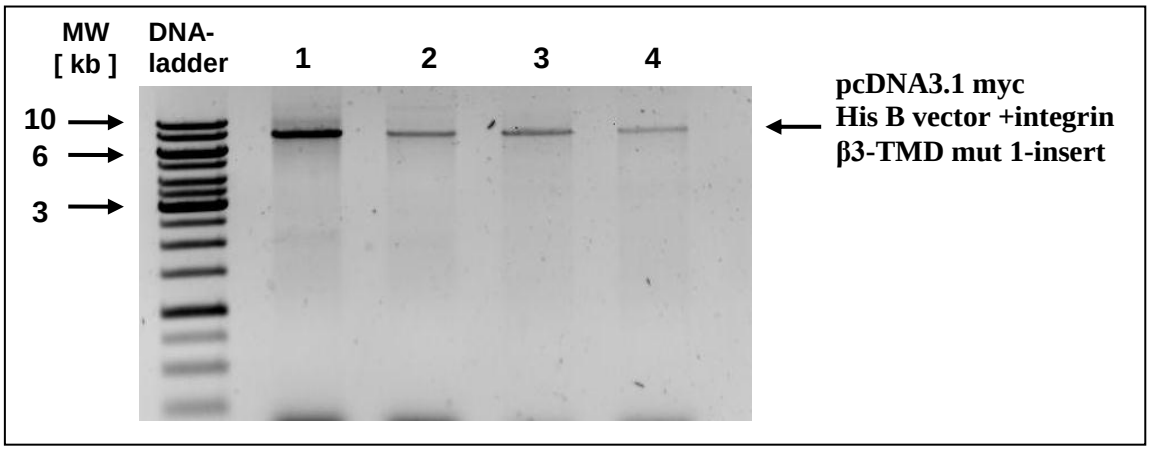

Figure 15 Agarose gel electrophoresis of the PCR product from the first integrin β3-TMD mutagenesis step.
Agarose gel electrophoresis performed on non-digested and Dpn I-digested plasmid cDNA encoding integrin β3-TMD mut 1. 10µl of non-digested and Dpn I-digested plasmid DNA mixed with 5 x loading buffer were run on 1% (w/v) agarose (lanes 1-4). MW shows molecular weight (PecGold 1 kb DNA ladder). One DNA fragment of 7.9 kb in size represents the vector for pcDNA3.1 myc His B vector (5.5 kb) plus the integrin β3 cDNA mut 1-insert (2.4 kb). (lane 1, lane 2 non-digested; lane 3, lane 4 Dpn I-digested, lane 1, lane 3: 1% (v/v) DMSO; lane 2, lane 4: 8% (v/v) DMSO)

E. coli were transformed with DNA, product of the Dpn I digestion step (see 2.2.2 d) and spread on agarose plates. 10 to 20 bacterial colonies were picked from the agar plates and the DNA was isolated and analysed by restriction digestion (see 2.2.3 a, d). In order to prove successful mutagenesis plasmid DNA encompassing the coding β3-TMD mut 1 was digested with the restriction enzyme Bcl I (target sequence: 5´-T/GATCA-3´). The restricted DNA fragments were then controlled using agarose gel electrophoresis (data not shown), knowing that Bcl I digestion of:

i) pcDNA3.1 myc His B containing cDNA insert encoding the wild type β3 integrin give rise to two DNA fragments observed at 1091 bp and 6809 bp, and

ii) pcDNA3.1 myc His B containing cDNA insert encoding the mutated TMD β3 integrin give rise to three DNA fragments of: 300 bp, 1091 bp, and 6482 bp.

The success of the first integrin β3-TMD mutagenesis step was further controlled by DNA sequencing (Sigma-Aldrich, Germany) and resulted in confirmation of correct DNA sequence.

II. Second mutation step: generation of integrin β3-TMD mut 2

In this second reaction, we exchanged amino acids: S699G; G702A; A703G; I704V from integrin β3-TMD into GpA-TMD (Figure 16).

aa number	699	700	701	702	703	704
β3 aa	S/G	V	M	G	A	I
β3 nt	gca	gtg	atg	ggg	gcc	att
GpA aa	G			A	G	V
GpA nt	gga			gcg	ggc	gtt

Figure 16 Design of the second integrin β3-TMD mutagenesis step.
Amino acid and the nucleotide sequences of integrin β3-TMD after the first mutation step are depicted. In the second mutagenesis step amino acid: S699G; G702A; A703G; I704V from integrin β3-TMD into GpA-TMD were exchanged.
aa: amino acid
nt: nucleotide
integrin β3-TMD amino acids and nucleotides to be mutated
GpA amino acids
nucleotides to be mutated
mutated nucleotide

For the second mutagenesis reaction the following primers were designed:

- β3-TMD 2.mut forward:
  5´-GGTGATCATCTTCGGAGTGATGGCGGGCGTTCTGCTCATTGG-3´
- β3-TMD 2.mut reverse:
  5´-CCAATGAGCAGAACGCCCGCCATCACTCCGAAGATGATCACC-3´

The melting temperature of the primers was calculated to 79.3°C.

As template for the second mutagenesis reaction served the expression vector pcDNA3.1 myc His B containing as insert the integrin β3-TMD mut 1. The PCR mixture was prepared as described (see 2.2.2 b). 8% (v/v) of DMSO was added to inhibit secondary structure formation of the template DNA. 0.5 µg/µl of BSA was used in the reaction mix

as a carrier to promote the stabilisation of very small concentrations of proteins/enzymes contained in the buffer, and for example to inhibit their precipitation at the tube wall.

The PCR cycles were chosen as follows:

Step 1. initial DNA denaturation	1 min at 95°C	
Step 2. denaturation	1 min at 95°C	18 cycles
Step 3. annealing	1 min at 55°C	
Step 4. elongation	9 min at 68°C	
Final step	5 min at 68°C	

The parental non-mutated methylated plasmid DNA was subjected to Dpn I digestion. The PCR products were checked by agarose gel electrophoresis. One DNA fragment of 7.9 kb in size represents the vector for pcDNA3.1 myc His B vector (5.5 kb) plus the integrin β3-TMD mut 2-insert (2.4 kb) (data not shown).

E. coli were transformed with DNA, product of Dpn I digestion step and spread on agarose plates. 10 bacterial colonies were picked from the agar plates and the DNA was isolated and analysed by restriction digestion. The restricted DNA fragments were checked by agarose gel electrophoresis. Two DNA fragments were observed, one of 5.5 kb for pcDNA3.1 myc His B vector, the other of 2.4 kb for the integrin β3 cDNA-insert (Figure 17).

The success of the second integrin β3-TMD mutagenesis step was further controlled by DNA sequencing on three selected clones (Sigma-Aldrich, Germany) and resulted in confirmation of correct DNA sequence.

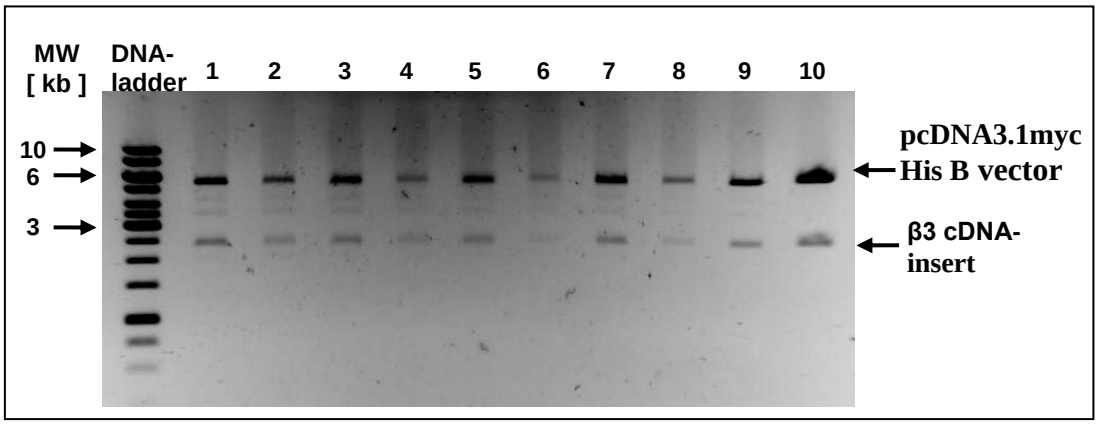

Figure 17 Agarose gel electrophoresis of the EcoR V and Xba I digested products from the second integrin β3-TMD mutagenesis step.
Agarose gel electrophoresis performed on EcoR V and Xba I digested plasmid cDNA encoding integrin β3-TMD mut 2. 5 U of EcoR V and Xba I digested plasmid DNA mixed with 5 x loading buffer were applied on 1% (w/v) agarose gel (lanes 1-10). MW shows molecular weight (PecGold 1kb DNA ladder). In lane 1-10 two DNA fragments can be observed, one fragment corresponds to the open plasmid (5.5 kb), the other correspond to the integrin β3 cDNA-insert (2.4 kb).

III. Third mutation step: generation of integrin β3-TMD mut 3

In this third reaction, we exchanged amino acids: L705I; L706G; I707T; G708I; and A710L from integrin β3-TMD into GpA-TMD (Figure 18).

aa number	705	706	707	708	709	710
β3 aa	L	L	I	G	L	A
β3 nt	ctg	ctc	att	ggc	ctt	gcc
GpA aa	I	G	T	I		L
GpA nt	atc	ggc	act	atc		ctc

Figure 18 Design of the third integrin β3-TMD mutagenesis step.
Amino acid and the nucleotide sequence of integrin β3-TMD after the second mutation step are depicted. In the third mutagenesis step amino acid: L705I; L706G; I707T; G708I; and A710L from integrin β3-TMD into GpA-TMD were exchanged.
aa: amino acid
nt: nucleotide
integrin β3-TMD amino acids and nucleotides to be mutated
GpA amino acids
nucleotides to be mutated

For the third mutagenesis reaction the following primers were designed:

- β3-TMD 3.mut forward:

  5´-GGAGTGATGGCGGGCGTTATCGGCACTATCCTTCTCGCCCTGCTCATCTGG-3´

- β3-TMD 3.mut reverse:

  5´-CCAGATGAGCAGGGCGAGAAGGATAGTGCCGATAACGCCCGCCATCACTCC-3´

The melting temperature of the primers was calculated to 75.7°C.

As template for the third mutagenesis reaction served the expression vector pcDNA3.1 myc His B containing as insert the integrin β3-TMD mut 2. The PCR mixture was prepared as described (see 2.2.2 b). 8% (v/v) of DMSO was added to inhibit secondary structure formation of the template DNA. The PCR cycles were equal to the cycles described above (see first and second mutagenesis reactions). In order to allow the perfect hybridisation for the mutagenesis oligodeoxynucleotide primers to their respective template DNA, two annealing temperatures were programmed, once at 54°C and once at 55°C, calculated to be about 20°C below the melting temperature of the oligodeoxynucleotide primers. PCR products were then digested with Dpn I in order to remove the non-mutated, methylated parental DNA. The PCR products were checked by agarose gel electrophoresis. One DNA fragment of 7.9 kb in in size represents the vector for pcDNA3.1 myc His B vector (5.5 kb) plus the integrin β3-TMD mut 3-insert (2.4 kb) (data not shown).

The success of the third integrin β3-TMD mutagenesis step was further controlled by DNA sequencing on two selected clones (Sigma-Aldrich, Germany) and resulted in confirmation of correct DNA sequence. Selection of clones followed the same steps used in the first and the second mutagenesis reaction described above (see generation of integrin β3-TMD mut 1 and integrin β3-TMD mut 2).

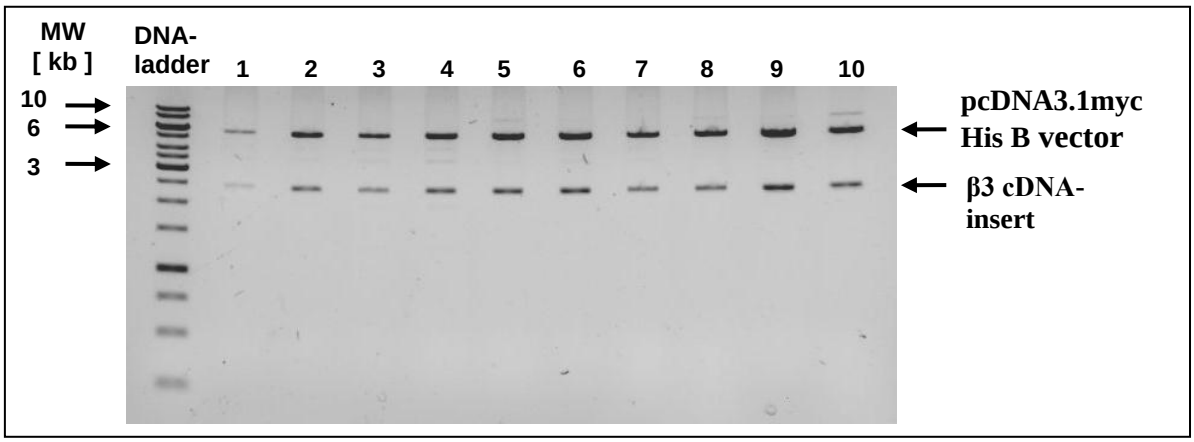

Figure 19 Agarose gel electrophoresis of the EcoR V and Xba I digested products from the third integrin β3-TMD mutagenesis step.
Agarose gel electrophoresis performed on EcoR V and Xba I digested plasmid cDNA encoding integrin β3-TMD mut 3. 5 U of EcoR V and Xba I digested plasmid DNA mixed with 5 x loading buffer were applied on 1% (w/v) agarose gel (lanes 1-10). MW shows molecular weight (PecGold 1kb DNA ladder). In lane 1-10 two DNA fragments can be observed; one fragment corresponds to the open plasmid (5.5 kb), the other correspond to the integrin β3 cDNA-insert (2.4 kb).
(PCR mixture medium containing 8% (v/v) of DMSO, PCR annealing temperature 54°C).

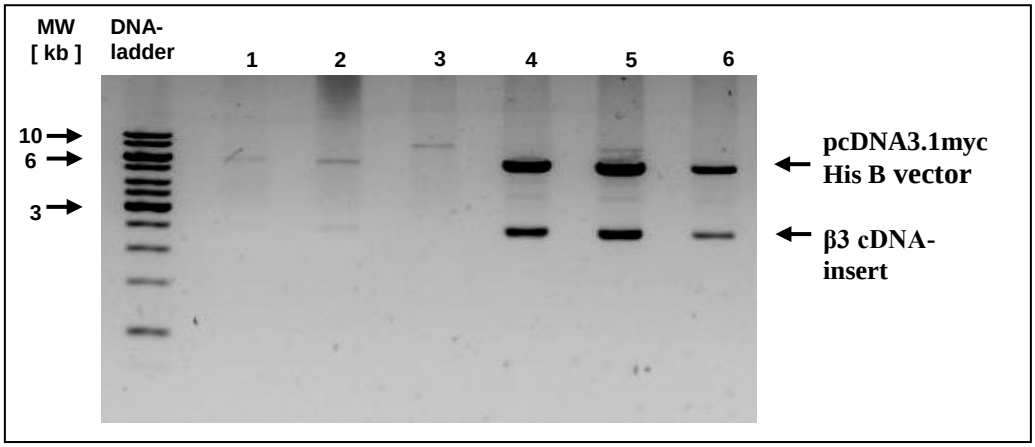

Figure 20 Agarose gel electrophoresis of the EcoR V and Xba I digested products from the third integrin β3-TMD mutagenesis step.
Agarose gel electrophoresis performed on EcoR V and Xba I digested plasmid cDNA encoding integrin β3-TMD mut 3.5 U of EcoR V and Xba I digested plasmid DNA mixed with 5 x loading buffer were applied on 1% (w/v) agarose gel (lanes 1-6). MW shows molecular weight (PecGold 1kb DNA ladder). In lane 1-6 two DNA fragments can be observed; one fragment corresponds to the open plasmid (5.5 kb), the other correspond to the integrin β3 cDNA-insert 2.4 kb.
(PCR mixture medium containing 8% (v/v) of DMSO, PCR annealing temperature 55°C).

IV. Fourth mutation step: generation of integrin β3-TMD mut 4

In the fourth mutagenesis reaction, we exchanged the following amino acids: L694T, and V695L from integrin β3-TMD into GpA-TMD (Figure 21).

aa number	693	694	695
β3 aa	I	L	V
β3 nt	atc	ctg	gtg
GpA aa		T	L
GpA nt		acg	ctg

Figure 21 Design of the fourth integrin β3-TMD mutagenesis step.
Amino acid and the nucleotide sequences of integrin β3-TMD after the third mutation step are depicted. In the fourth mutagenesis step amino acid L694T, and V695L from integrin β3-TMD into GpA-TMD were exchanged.
aa: amino acid
nt: nucleotide
integrin β3-TMD amino acids and nucleotides to be mutated
GpA amino acids
nucleotides to be mutated

For the fourth mutagenesis reaction the following primers were designed:

- β3-TMD 4 forward primer:

  5´-CCCTGACATCACGCTGATCATCTTCGGAGTGATGG-3´

- β3-TMD 4 reverse primer:

  5´-CCATCACTCCGAAGATGATCAGCGTGATGTCAGGG-3´

The melting temperature of the primers was calculated to 76°C.

As template for the fourth mutagenesis reaction served the expression vector pcDNA3.1 myc His B containing as insert the integrin β3-TMD mut 3. The PCR cycles were equal to the cycles described above (see first, second, and third mutagenesis reactions). Two annealing temperatures were programmed once at 55°C and once at 57°C. The PCR products were then digested with Dpn I in order to remove the non-mutated, methylated parental DNA. Amplified template DNA were checked by agarose gel electrophoresis. One DNA fragment of 7.9 kb in size represents the vector for pcDNA3.1 myc His B vector (5.5 kb) plus the integrin β3 cDNA mut 4-insert (2.4 kb) (Figure 22).

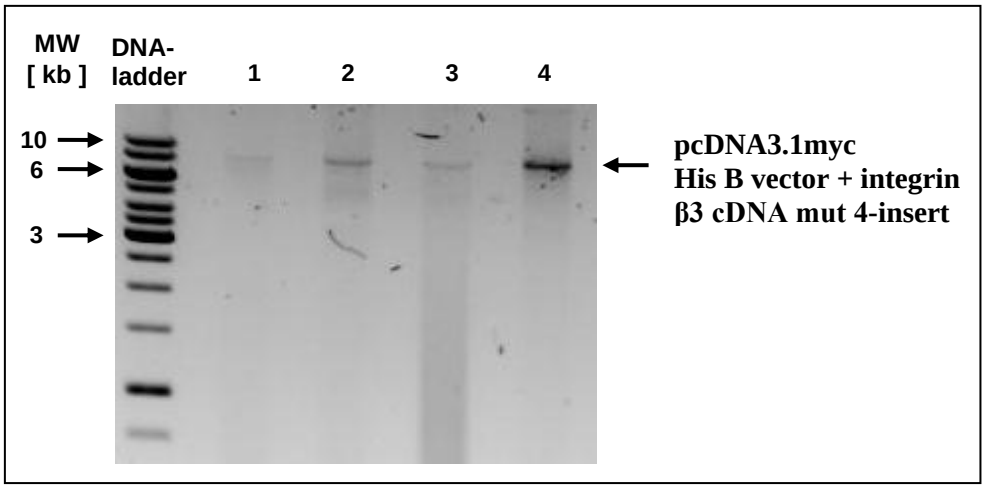

Figure 22 Agarose gel electrophoresis of the PCR product from the fourth integrin β3-TMD mutagenesis step.
Agarose gel electrophoresis performed on Dpn I digested plasmid cDNA encoding integrin β3-TMD mut 4. 10µl of Dpn I digested plasmid DNA mixed with 5 x loading buffer were applied on 1% (w/v) agarose gel (lanes 1-4). MW shows molecular weight (PecGold 1kb DNA ladder). One DNA fragment of 7.9 kb in size represents the vector for pcDNA3.1 myc His B vector (5.5 kb) plus the integrin β3 cDNA mut 4-insert (2.4 kb). (lane 1& lane 2: PCR annealing temperature by 55°C; lane 3& lane 4: PCR annealing temperature 57°C)

The success of the fourth integrin β3-TMD mutagenesis step was further controlled by DNA sequencing on two selected clones and resulted in confirmation of correct DNA sequence. Selection of clones followed the same steps used in the first, second, and third mutagenesis reaction described above.

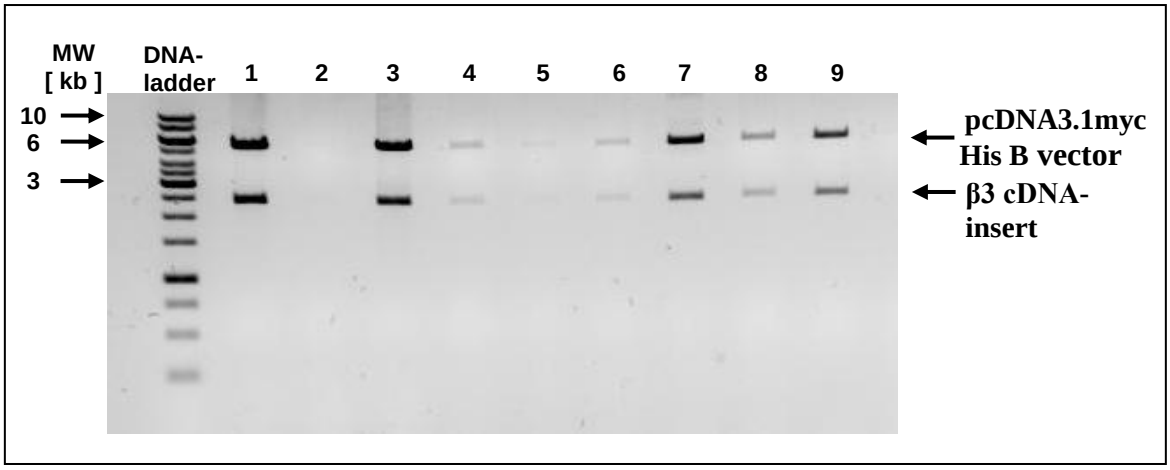

Figure 23 A) Agarose gel electrophoresis of the EcoR V and Xba I digested products from the fourth integrin β3-TMD mutagenesis step.
Agarose gel electrophoresis performed on EcoR V and Xba I digested plasmid cDNA encoding integrin β3-TMD mut 4. 5 U of EcoR V and Xba I digested plasmid DNA mixed with 5 x loading buffer were applied on 1% (w/v) agarose gel (lanes 1-9). MW shows molecular weight (PecGold 1kb DNA ladder). In lane 1-9 two DNA fragments can be observed; one fragment corresponds to the open plasmid (5.5 kb), the other correspond to the β3 cDNA-insert (2.4 kb).

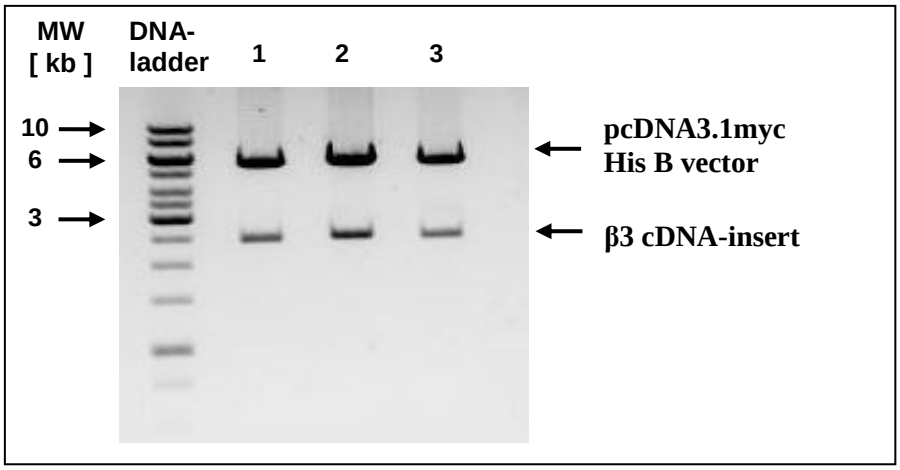

Figure 23 B) Agarose gel electrophoresis of the EcoR V and Xba I digested products from the fourth integrin β3-TMD mutagenesis step.
Agarose gel electrophoresis performed on EcoR V and Xba I digested plasmid cDNA encoding integrin β3-TMD mut 4. MW shows molecular weight (PecGold 1kb DNA ladder). In lane 1-3 shows the result from isolated plasmid DNA clones 10, 11, and 12: two DNA fragments can be observed; one fragment corresponds to the open plasmid (5.5 kb), the other correspond to the β3 cDNA-insert (2.4 kb).

3.1.3.2 Generation of a point mutated GxxxG motif of the glycophorin A transmembrane domain to GxxxI

As a control, we generated TMD-GpA-I construct. For this, the central motif of the TMD-GpA (GxxxG) construct was exchanged to the TMD-GpA-I (GxxxI) (Figure 24). This point mutation allows the transmission from strong interacting TMD-helices to non-interacting helices as previously shown in the context of the GpA-homodimer (Lemmon et al., 1992, 7683-7689).

This mutation was realised using the following primers:

- β3-TMD-ILE forward primer:
  5´-GCTGATCATCTTCGGAGTGATGGCGATCGTTATCGGC-3´
- β3-TMD-ILE reverse primer:
  5´-GCCGATAACGATCGCCATCACTCCGAAGATGATCAGC-3´

The melting temperature for the primers was calculated according to the appropriate formula (see 2.2.2 a) to 80°C. As template for this mutagenesis reaction served the expression vector pcDNA3.1 myc His B containing as insert the β3-TMD mut 4. 8% (v/v) of DMSO was added to inhibit secondary structure formation of the template DNA. The PCR cycles were equal to the cycles used for the fourth TMD-GpA mutagenesis steps. In order to allow the perfect hybridisation for the mutagenesis oligodeoxynucleotide primers

to their respective template DNA two annealing temperatures were programmed, once at 55°C and once at 57°C. PCR products were then digested with Dpn I in order to remove the non-mutated, methylated parental DNA. The amplified template DNA was checked by agarose gel electrophoresis. One DNA fragment of 7.9 kb in size represents the vector for pcDNA3.1 myc His B vector (5.5 kb) plus the integrin β3 cDNA-insert (2.4 kb) (Figure 25).

TMD-GpA:

^{693}ITLIIFGVMAGVIGTIL^{710}L

GxxxG-motif

aa number	699	700	701	702	703
GpA aa	G	V	M	A	G
	gly	val	met	ala	gly
GpA nt	gga	gtg	atg	gcg	ggc

TMD-GpA-I:

^{693}ITLIIFGVMAIVIGTIL^{710}L

GxxxI-motif

aa number	699	700	701	702	703
mut aa	G	V	M	A	I
	gly	val	met	ala	ile
mut nt	gga	gtg	atg	gcg	atc

Figure 24 Sequence of TMD-GpA and TMD-GpA-I. Amino acid and the nucleotide sequences of TMD-GpA generated by the previous four mutagenesis reactions are depicted. In this mutagenesis step, we exchanged amino acid: G703I from TMD-GpA (dimerization motif GxxxG) into TMD-GpA-I (dimerization motif GxxxI).
aa: amino acid
nt: nucleotide
amino acid and nucleotide to be mutated
nucleotides to be mutated
GxxxG motif

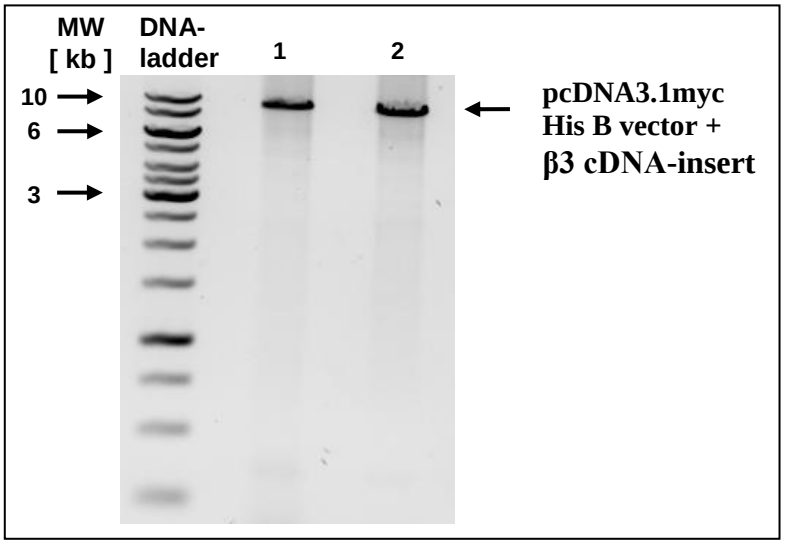

Figure 25 Agarose gel electrophoresis of the PCR product from the point mutated GxxxG motif of the GpA-TMD to GxxxI.
Agarose gel electrophoresis performed on Dpn I digested plasmid cDNA encompassing TMD-GpA-I mutant. 10µl of Dpn I-digested plasmid DNA mixed with 5 x loading buffer were applied on 1% (w/v) agarose gel (lanes 1 and 2). MW shows molecular weight (PecGold 1kb DNA ladder). One DNA fragment revealed a size of 7.9 kb in accordance with the plasmid pcDNA 3.1 myc His B encompassing TMD-GpA-I mutant. (lane 1: PCR annealing temperature by 55; lane 2: PCR annealing temperature 57 °C).

The sequence of the mutated cDNA inserts encompassing TMD-GpA-I mutant was controlled by Sigma-Aldrich (Germany) on two selected clones. Selection of the clones followed the same steps used for the generation of TMD-GpA mutant (see 3.1.3.1). Both DNA plasmids were confirmed to contain the Isoleucin (Ile703) point mutation.

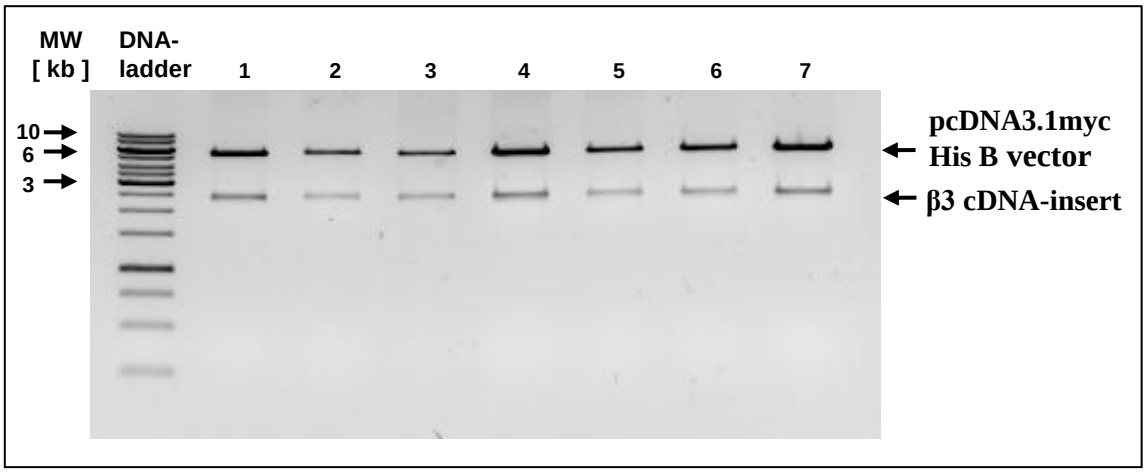

Figure 26 Agarose gel electrophoresis of the EcoR V and Xba I digested products from pcDNA 3.1 myc His B expression vector encoding TMD-GpA-I.
Agarose gel electrophoresis performed on EcoR V and Xba I digested plasmid cDNA encoding TMD-GpA-I mutant. MW shows molecular weight (PecGold 1kb DNA ladder). In lane 1-7 two DNA fragments can be observed; one fragment corresponds to the open plasmid (5.5 kb); the other correspond to the β3 cDNA-insert (2.4 kb).

3.2 Establishment of human ovarian cancer cell transfectants expressing either wild type or distinct mutant forms of integrin αvβ3

As stable cell transfection system, the human ovarian cancer cell line OV-MZ-6 was chosen, knowing that they display low endogenous integrin αvβ3 expression levels (Hapke et al., 2003, 1073-1083). Transfections of OV-MZ-6 cells with the successfully generated different integrin αv/β3 cDNA constructs were conducted in collaboration with Dr. Martina Müller, Clinical Research Unit, Dept. of Obstetrics & Gynecology, Technische Universität München.

The following OV-MZ-6 cell transfectants were established to study the impact of TMD conformation (clasped/unclasped) and cytoplasmic salt bridge formation on integrin αvβ3 activation:

Salt bridge:

OV-MZ-6 cell transfectants	αv	β3	salt bridge formation
OV-αvβ3D723R	αv-WT	$\beta3_{D723R}$	no
OV-αvR995Dβ3D723R	αv_{R995D}	$\beta3_{D723R}$	possible charge reversal salt bridge
OV-αvR995Dβ3	αv_{R995D}	β3-WT	no
OV-αvβ3	αv-WT	β3-WT	yes

Transmembrane domain:

OV-MZ-6 cell transfectants	αv	β3	TMD conformation
OV-TMD-GpA	αv-TMD-GpA	β3-TMD-GpA	TMD clasping
OV-TMD-GpA-I	αv-TMD-GpA-I	β3-TMD-GpA-I	TMD separation

Wild type:

OV-MZ-6 cell transfectants	αv	β3
OV-αvβ3	αv-WT	β3-WT

Vector:

OV-MZ-6 cell transfectants	vector
OV-VEC	pcDNA3.1 His B vector

3.2.1 Immunocytochemical detection of the content of integrin αvβ3 and its variants in transfected human ovarian cancer cells

For characterisation of successful cell transfection, various different cell clones of each transfection category were stained for integrin αvβ3 by using the monoclonal antibody #LM609 directed to the heterodimer integrin αvβ3. Signal detection was carried out by using an Alexa-488-conjugated goat anti-mouse IgG. Immunostaining of cells was evaluated by confocal laser scanning microscopy (CLSM).
We selected clones with very similar cellular expression levels of integrin αvβ3 which enable us to compare the results in cell experiments among the different cell transfectants.

3.3 Integrin αvβ3-mediated cell proliferation as a function of its transmembrane domain sequence

We studied the effect of TMD variants of integrin αvβ3 on the proliferative activity of OV-MZ-6 cancer cells. Hapke and co-workers observed that the proliferation of human ovarian OV-MZ-6 cancer cells is under the control of integrin αvβ3 (Hapke et al., 2003, 1073-1083). Thus, in the present study we were interested in the role of the conformation of the TMD of integrin αvβ3 on OV-MZ-6 cell proliferation. To that aim, cells expressing TMD mutants (TMD-GpA and TMD-GpA-I) were seeded at a density of 10,000 cells/well into 96-well cell culture plates. MTT assay was performed as described above (see 2.2.4 b). Cells expressing wild type integrin αvβ3 (TMD-αvβ3) to a similar extent served as control. Depicted is a representative experiment showing the cell proliferative activity after 24 h of incubation at 37°C/ 5% (v/v) CO_2 (Figure 28). The highest increase in cell numbers was observed by cells expressing the TMD-GpA-I mutant, displaying TMD dissociation. In contrast, cell transfectants expressing the TMD-GpA mutant with clasped TMD showed significantly reduced proliferative activity (Figure 28). Cells expressing TMD-αvβ3 wild type disclosed an intermediate cell proliferation rate.
Parallel to the MTT assays, cell proliferative activity was determined by cell counting in a Neubauer hemocytometer. For this, cell clones from each transfection category (TMD-αvβ3, TMD-GpA, TMD-GpA-I, VEC) were seeded at a density of 20,000 cells/well into

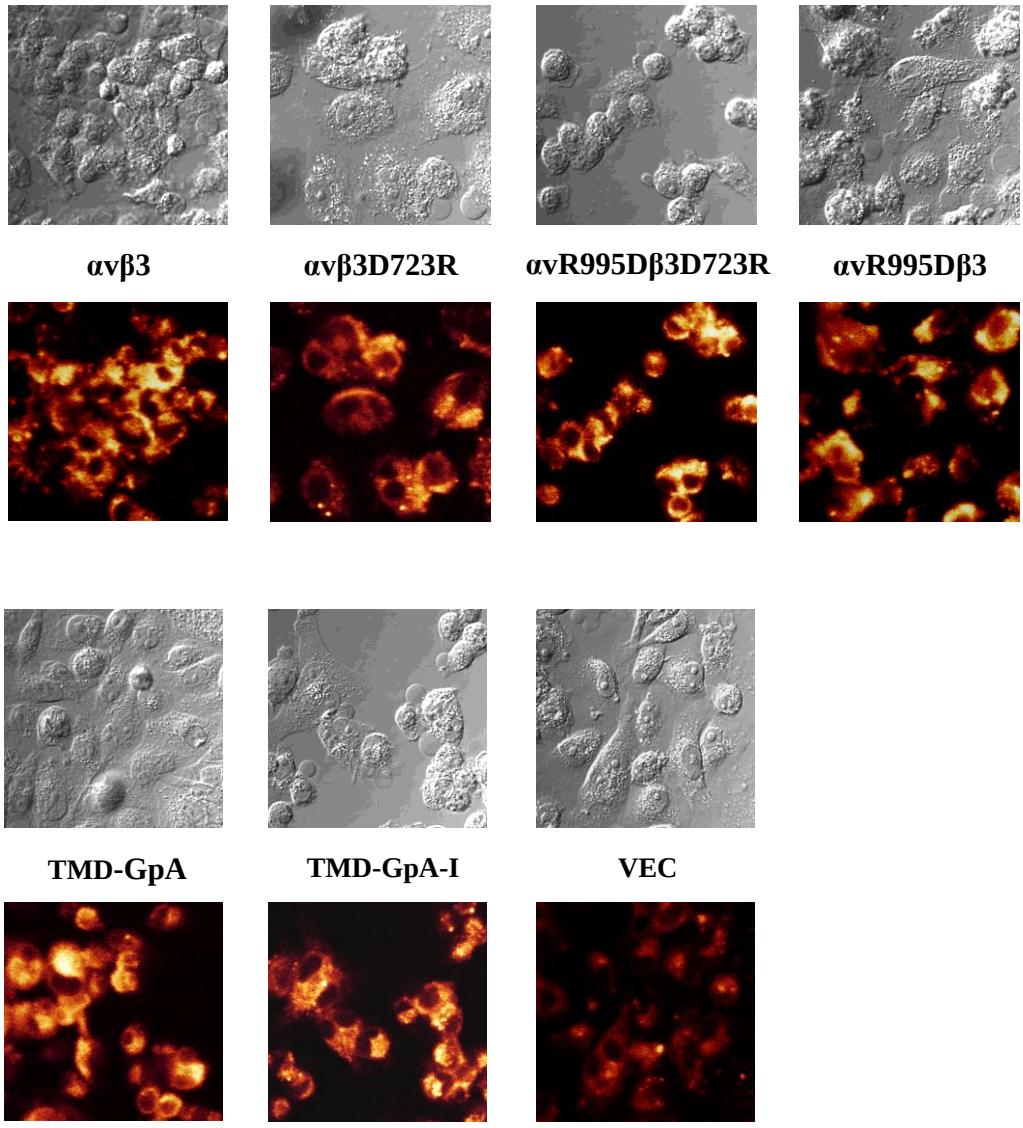

Figure 27 Immunocytochemical detection of integrin αvß3 and its mutated variants in transfected OV-MZ-6 cells.
Expression levels of integrin αvß3 in cells transfected to express integrin αvß3 having a salt bridge mutation (OV- $\alpha v\beta 3_{D723R}$; $\alpha v_{R995D}\beta 3_{D723R}$; $\alpha v_{R995D}\beta 3$), or carrying mutation in the TMD (OV-TMD-GpA; OV-TMD-GpA-I), when compared to OV-MZ-6 cells overexpressing αvß3-WT or vector-transfected cells (VEC). All cell clones were primary stained with mAb #LM609 directed to integrin αvß3 and secondary with Alexa-488-conjugated goat anti-mouse IgG. Representative fluorescence images together with the corresponding differential interference contrast images are described. Fluorescence staining intensity: low (red), medium (yellow), and high (white) (images are kindly provided by Dr. Martina Müller).

96-well cell culture plates. The numbers of viable cells were counted every other 12 h over a time period of 60 h. Depicted is a representative experiment showing the cell proliferative activity during a time course (Figure 29 A). The highest increase in cell number was observed for cells expressing TMD-GpA-I, followed by TMD-αvβ3 and TMD-GpA. Vector-transfected cells showed the lowest proliferative activity. The cell count determined at 60 h is represented as a histogram in figure 29 B. The proliferative activity of cells expressing TMD-GpA-I, TMD-αvβ3, TMD-GpA, respectively, is compared to the cell number of vector-transfected cell clones. Cell expressing TMD-GpA-I proliferate up to 2-folds stronger, cells containing TMD-αvβ3 proliferate up to 1.8-folds stronger and cells with TMD-GpA up to 1.5-folds stronger compared to vector.

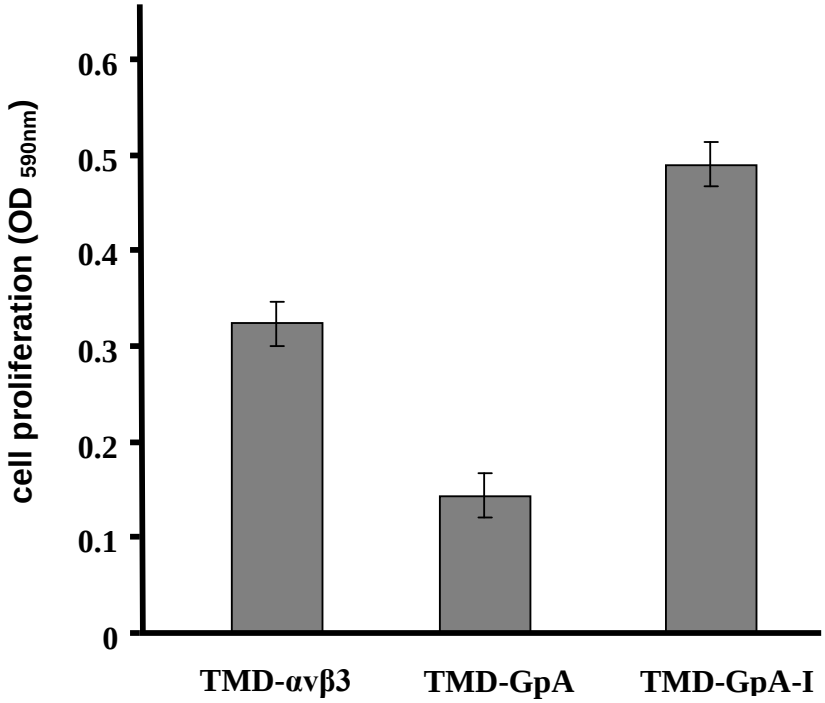

Figure 28 OV-MZ-6 cell proliferation as a function of integrin αvβ3-TMD conformation.
Cell proliferative activity was determined by MTT assay. For this, TMD- αvβ3 (wild type), TMD-GpA (strong TMD dimerization), and TMD-GpA-I (abrogated TMD dimerization) transfected OV-MZ-6 cell clones, respectively, were seeded at a density of 10,000 cells/well into 96-well cell culture plates and cultivated for 24 h. Cells overexpressing TMD-GpA-I showed strongest proliferation compared to cells expressing TMD-αvβ3. Cell proliferation of cells expressing the TMD-GpA mutant was markedly reduced when compared to TMD-αvβ3-transfected control cell clones. We detected strong proliferation difference between the two TMD mutated cell clones. Cells containing TMD-GpA-I construct proliferated up to 3-folds stronger compared to cells containing the TMD-GpA construct. Data represent the absorbance of 590 nm using ELISA reader and are directly proportional to the number of viable cells. Mean values (± SD) of a representative experiments are shown (n = 3, ± S.D.).

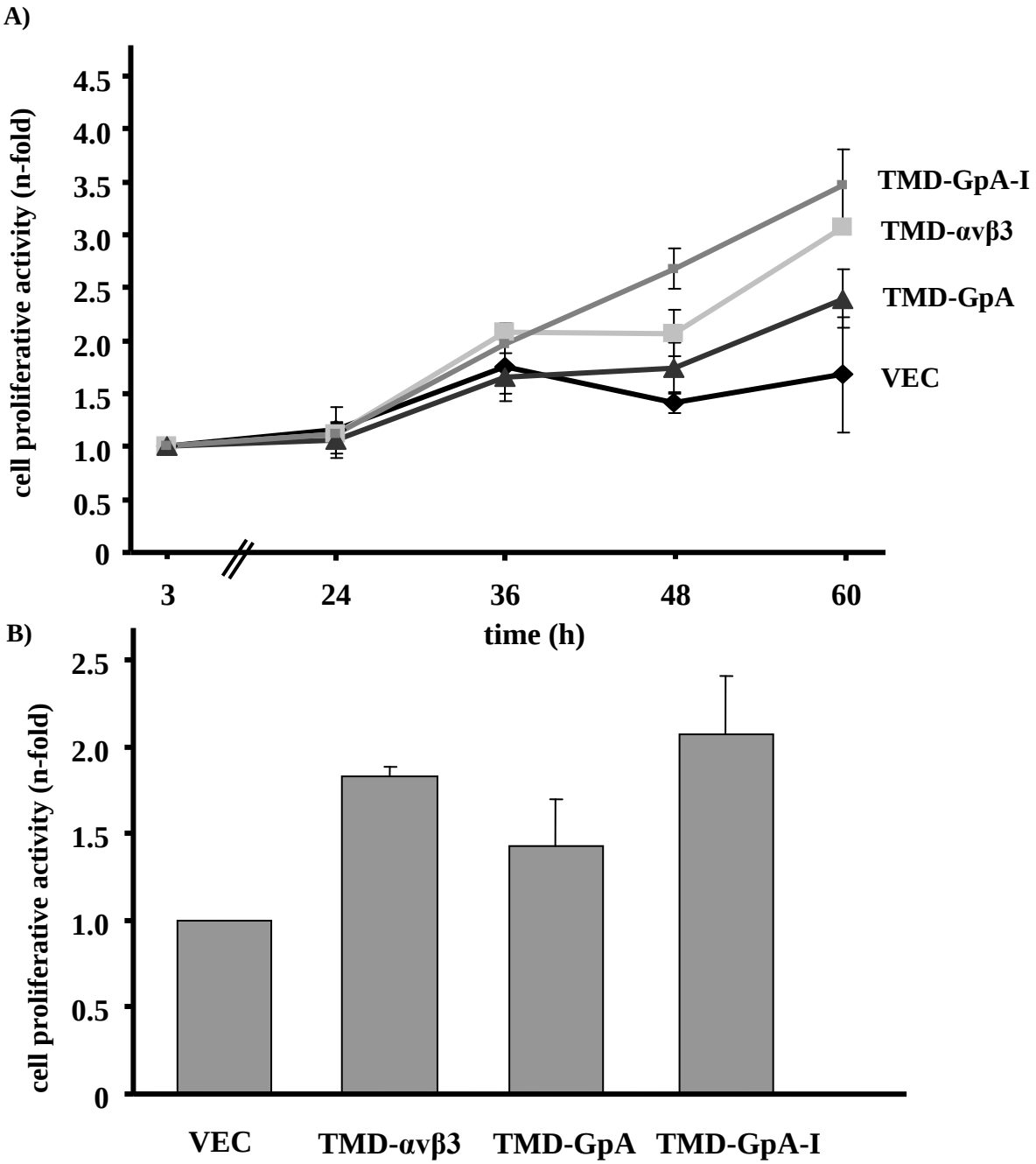

Figure 29 OV-MZ-6 cell proliferation as a function of integrin αvβ3-TMD conformation. OV-MZ-6 cells containing TMD-αvβ3, TMD-GpA, TMD-GpA-I, and vector-transfected cells, respectively, were seeded at a density of 20,000 cells/well into 12-well cell culture dishes in 1 ml of DMEM, 10% (v/v) FCS. A) After 24, 36, 48, and 60 h of cultivation, cell numbers were counted upon trypan blue exclusion using the Neubauer hemocytometer. The highest increase in cell number was archieved by cells expressing TMD-GpA-I, followed by TMD- αvβ3 and TMD-GpA. Vector-transfected cells showed the lowest proliferative activity. Data are given as mean values (± SD) of representative experiments as "n-fold" by setting the cell numbers at 3 h of adhesion to "1" (n = 3, ± S.D.). B) Evaluation of number of viable cells by counting after 60 h of cell cultivation. Cell expressing TMD-GpA-I proliferate up to 2-fold stronger, cells containing TMD-αvβ3 proliferate up to 1.8-fold stronger and cells with TMD-GpA up to 1.5-fold stronger compared to vector. Data are given as mean values (± SD) of representative experiments as "n-fold" by setting the number of vector-transfected cells to "1" (n = 3, ± S.D.).

3.4 Cooperation between integrin αvβ3 and the epidermal growth factor receptor

Lössner and co-workers showed in OV-MZ-6 cells that expression of the epidermal growth factor receptor (EGF-R) and its activated and thus phosphorylated form, p-EGF-R, is under the control of integrin αvβ3 (Lössner et al., 2008, 2746-2761). The authors revealed integrin αvβ3-dependent upregulation of EGF-R activity and expression. Knowing that, we were interested to investigate the impact of the integrin TMD conformation on (p-)EGF-R protein expression.

3.4.1 Epidermal growth factor receptor expression as a function of the integrin αvβ3 transmembrane domain sequence

We investigated the effect of the integrin αvβ3-TMD conformation and thus its activity state on the p-EGF-R/ EGF-R protein expression levels. For the detection of the activated p-EGF-R, 100,000 cells of each transfection category were harvested, fixed in 4% (w/v) PFA and blocked in 2% (w/v) BSA (see 2.2.5 a). Cells were then incubated with mAb directed to the p-EGF-R followed by the addition of an Alexa-488-conjugated goat anti-mouse IgG. We observed a significant, up to 2.5-fold elevated p-EGF-R expression in OV-MZ-6 cells expressing the integrin αvβ3 TMD-GpA mutant compared to vector-transfected cells. On the contrary, OV-MZ-6 cells expressing the TMD-GpA-I mutant did not significantly enhance p-EGF-R protein expression (Figure 30).
Moreover, with respect to the total EGF-R expression, we observed an up to 2-fold elevated expression in TMD-GpA-transfected cells compared to vector-transfected cells. In TMD-GpA-I-transfected cells EGF-R-expression levels were not significantly altered (Figure 30).

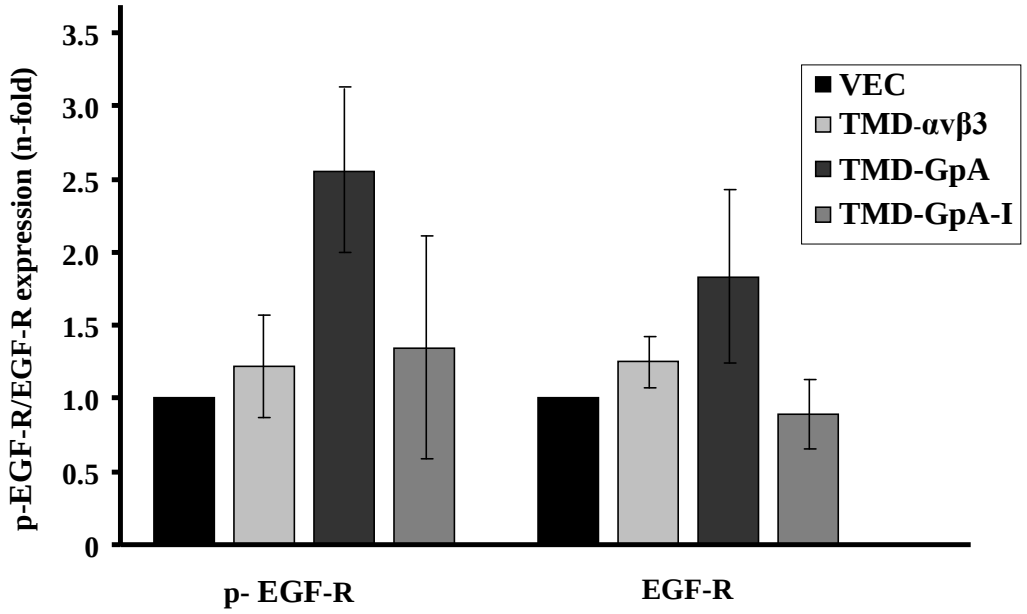

Figure 30 Detection of p-EGF-R/EGF-R expression in OV-MZ-6 cells as a function of integrin αvβ3-TMD conformation.

p-EGF-R/EGF-R expression was determined by FACS analysis as described. Vector-, TMD-αvβ3-, TMD-GpA- and TMD-GpA-I-transfected OV-MZ-6 cells, respectively, were cultivated on 75 ml cell culture flasks until cell monolayers reached a confluency of approximately 70%.

For the detection of activated p-EGF-R, 100,000 cells of each transfection category were harvested, fixed in 4% (w/v) PFA, and then blocked in 2% (w/v) BSA (see 2.2.5 a). Cells were incubated with mAb directed to the p-EGF-R followed by secondary Alexa-488-conjugated goat anti-mouse IgG.

For detection of total EGF-R protein expression, cells were incubated with mAb directed to EGF-R followed by secondary Alexa-488-conjugated goat anti-mouse IgG. Flow cytofluorometrical analysis was performed by using the FACS-Calibur instrument (Becton-Dickinson). Data are given as mean values (± SD) of three independent experiments as "n-fold" by setting the expression level in vector-transfected cells to "1" (n = 3, ± S.D.).

3.4.2 Effect of epidermal growth factor on integrin αvβ3-dependant human ovarian cancer cell proliferation as a function of integrin transmembrane domain conformation

Lössner and co-workers showed that OV-MZ-6 cancer cells expressing integrin αvβ3 exhibit increased proliferation response to EGF stimulation, when compared to unstimulated cells (Lössner et al., 2008, 2746-2761). Knowing that, we investigated the effect of EGF on OV-MZ-6 cell proliferative activity as a function of the integrin αvβ3-TMD conformation. To that aim, OV-MZ-6 cells transfected to express integrin αvβ3 variants of its TMD sequence (TMD-GpA and TMD-GpA-I) were tested regarding their proliferative response to exogenous EGF stimulation. For this, cells were washed in PBS and stimulated in DMEM, 1% (v/v) FCS including 20 ng/ml EGF. As a control, OV-MZ-6 cell transfectants were incubated in DMEM, 1% (v/v) FCS alone. After 24 h of incubation, cells were counted. Surprisingly, we did not detect significant increase in the proliferative activity of all OV-MZ-6 cell transfectants stimulated with EGF, when compared to OV-MZ-6 cells without EGF stimulation.

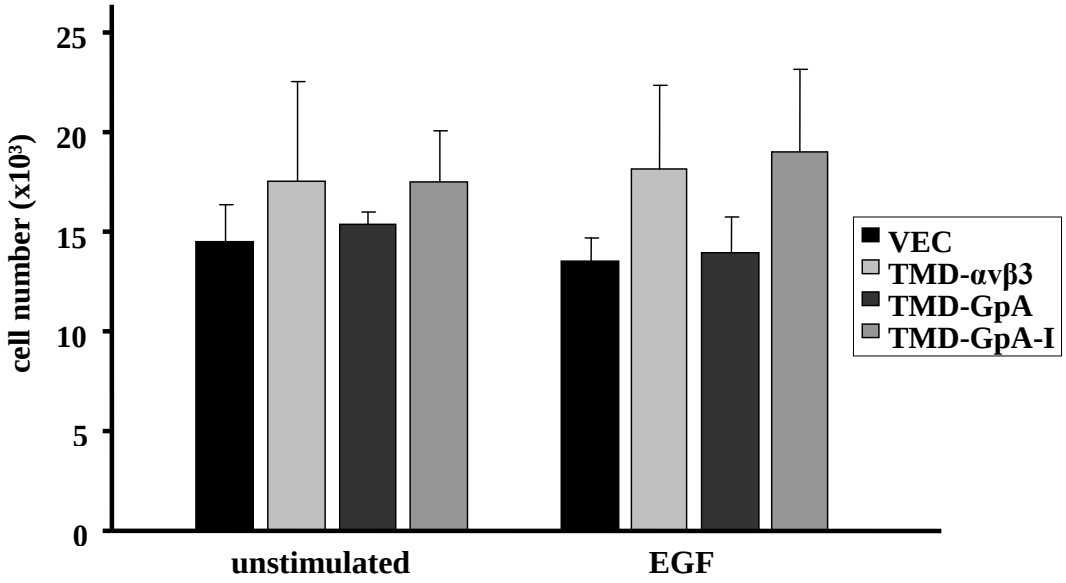

Figure 31 Evaluation of the proliferative response of OV-MZ-6 cancer cell lines containing various TMD conformations to EGF stimulation.
Vector-, TMD-αvβ3-, TMD-GpA- and TMD-GpA-I-transfected OV-MZ-6 cells, respectively, were passed into 12-well cell culture plates in DMEM, 1% (v/v) FCS. Cells were allowed to adhere for 3 h and then washed once in PBS. FCS-reduced medium (DMEM, 1% (v/v) FCS) was added to each cell culture. After 12 h of this starvation period, cells were stimulated by the addition of 20 ng/ml EGF. As control cells were incubated in the presence of DMEM, 1% (v/v) FCS alone. Cell numbers were counted after 24 h of incubation at 37°C/5% (v/v) CO_2. Data are given as mean values (± SD) of three independent experiments.

4 Discussion

Integrins are important for the physiological cell development, hemostasis, inflammation, angiogenesis, and immune responses (Bunch, 2010, 1841-1849). They play a central role in a series of cell biological events, such as migration, adhesion, proliferation, and differentiation (Giancotti, 1997, 691-700, Watt, 2002, 3919-3926, Al-Jamal and Harrison, 2008, 81-101). Integrins are known as well as an active mediator in pathological angiogenesis, cancer development and metastatic cell dissemination. Those adhesion receptors are capable of transmitting signals bidirectionally across the cell membrane and adopt distinct conformational states during their activation. However, the exact molecular/structural mechanisms of integrin activation and integrin-mediated signal transduction are still not fully resolved (Zhu et al., 2009, 234-249).

As a model integrin, we selected the tumor biologically relevant integrin αvβ3. The aim of the present study was first, to generate mutants of the integrin αvβ3 TMD and the cytoplasmic putative salt bridge, and second, to investigate the effect of the TMD mutants on the integrin αvβ3-dependant proliferative activity of OV-MZ-6 cells. The human ovarian cancer cell line OV-MZ-6 was transfected with expression vector encoding the different integrin αvβ3 cDNA constructs. Thus, cell transfectants were generated to express an integrin αvβ3 variant with strong TMD association (TMD-GpA construct; dimerization motif GxxxG), or the TMD-GpA-I construct, displaying unclasped TMD (dimerization motif GxxxI). The role of the integrin αvβ3 cytoplasmic salt bridge was investigated in OV-MZ-6 cells stably transfected to express integrin αvβ3 either capable of forming a putative salt bridge (wild type αvβ3 or a charge reversal mutant $\alpha v_{R995D}\beta 3_{D723R}$) or lacking this salt bridge ($\alpha v_{R995D}\beta 3$ or $\alpha v\beta 3_{D723R}$).

4.1 *In vitro* site-directed mutagenesis of integrin αvβ3

In order to generate integrin αvβ3 mutants by *in vitro* site-directed mutagenesis, we used the QuikChange™ kit (see 2.1.9). Compared to alternative site-directed mutagenesis methods, this kit is based on a quicker and easier protocol that gives rise to a large amount of mutated plasmid DNA. Double-stranded DNA is used as template which is easier to prepare compared to single stranded template DNA, used for example in the first developed single-primer method for site-directed mutation (Primose S., 2006, 141-156).

In the performed *in vitro* site-directed mutagenesis method, the oligodeoxynucleotide primers containing the desired mutation are extended during PCR by PfuTurbo DNA polymerase. This themostable PfuTurbo DNA polymerase is a high-fidelity polymerase, which compared to a low-fidelity Taq polymerase minimises the risk of spontaneous or random mutations (Primose S., 2006, 141-156). The PfuTurbo DNA polymerase has no strand displacement function, allowing the replication of plasmid DNA without removing the mutated oligodeoxynucleotide primers. Moreover, the QuikChange™ method has a digestion step using the restriction enzyme Dpn I. The parental DNA, derived from *E. coli* bacteria is methylated and thus sensitive to Dpn I endonuclease. Dpn I digests the parental methylated DNA, whereas the DNA produced by PCR is non-methylated and therefore resistant to Dpn I digestion. On the contrary, in the "single-primer" mutagenesis method, both methylated and non-methylated mutated double stranded DNA were transformed into *E. coli* wherein the cell mismatch repair system has the tendency to repair the non-methylated DNA. Therefore the introduced mutations are often eliminated giving rise to a very low yield of mutated progeny (Primose S., 2006, 141-156). The QuikChange™ method has overcome this problem associated with the mismatch repair system of *E. coli* by eliminating the parental DNA strand upon Dpn I restriction. This digestion step introduces nicks into the parental DNA that form with the newly synthesised mutated DNA a double stranded plasmid. After transformation into *E. coli*, the repair system is thus forced to repair the nicked parental DNA using the non-damaged mutated strain as a template.

The mutagenesis method is based on a rapid 4-step-procedure (Figure 10) allowing DNA amplification in a single day of work. Another advantage of this method is that it requires only a very small amount of DNA template. The high fidelity of PfuTurbo DNA polymerase and Dpn I restriction, both contribute to high mutagenesis efficiency and decrease potential random mutations. For the mutagenesis approach in the present work, we optimised the method in several regards: First, the concentration of the DNA template was titrated. For the conducted PCR the concentration of 50 ng of template DNA turned out to be the optimal concentration. Second, DMSO was added to the PCR mixture, particularly in a DNA template with high amount of GC. DMSO is known to avoid secondary structure formation, to interfere the self-complementarity of the DNA and to reduce the risk of interfering reactions. Hereby, it occurs that the concentration of DMSO is critical factor for this function. Hardjasa and co-workers studied the effect of 2% (v/v) DMSO in PCR and revealed no significant effect on the yield or the proportion of

mutations in the DNA progeny (Hardjasa, 2010, 161-164). For the present PCR, we titrated the concentration of the DMSO. We used 8% (v/v) DMSO which turned out to be the optimal concentration for the conducted PCR. Third, BSA was used in the reaction mix as a carrier to promote the stabilisation of very small concentrations of proteins/enzymes contained in the buffer, and for example to inhibit their precipitation at the tube wall. Fourth, the PCR cycle conditions were varied, in order to allow the perfect hybridisation for the mutagenesis oligodeoxynucleotide primers to their respective template DNA. Temperatures between 24°C-17°C below the calculated melting temperature of the mutagenesis primers were used. It turned out that the optimum is by 24°C for the conducted PCR.

4.2 Impact of integrin cytoplasmic salt bridge formation on integrin αvβ3 activation

The cytoplasmic domain of integrins has been shown to adopt different conformational states that are supposed to be connected to the integrin activity state. However, the exact structural mechanisms are not yet completely defined. The functional role of a proposed cytoplasmic salt bridge formed between the conserved R995 of the α-subunit and D723 of the β-subunit is still a conflicting scientific matter (Hughes et al., 1996, 6571-6574, Czuchra et al., 2006, 889-899, Imai et al., 2008, 5007-5015). One one hand, the salt bridge appears to be important for integrin activation (Hughes et al., 1996, 6571-6574, Imai et al., 2008, 5007-5015). It is supposed that salt bridge formation keeps integrins in a resting, non-activated state, whereas separation of this interface activates the integrin receptor (Hughes et al., 1996, 6571-6574, Imai et al., 2008, 5007-5015). On the other hand, conflicting results concerning the role of the salt bridge for integrin activation have been reported. Czuchra and co-workers did not observe obvious differences in integrin activation, no matter if the salt bridge was formed or not. Thus, the authors concluded that the salt bridge might not be essential for integrin activation (Czuchra et al., 2006, 889-899).

In order to shed light on the role of this membrane-proximal cytoplasmic portion of integrin subunits for integrin activation and ligand binding affinity, we generated integrin αvβ3 mutants in which the salt bridge-forming amino acids were mutually exchanged (αv_{R995D}; $\beta 3_{D723R}$) in the individual integrin chains. In order to study the impact of such

mutants on integrin αvβ3-mediated biological function, the human ovarian cancer cell line OV-MZ-6 was chosen as a cellular expression system. As described above (see 3.2), OV-MZ-6 cells were stably transfected with different combinations of mutated αv- and β3-chains to express integrin αvβ3 variants capable of forming a putative salt bridge (wild type αvβ3 or a charge reversal mutant $\alpha v_{R995D}\beta 3_{D723R}$) or wherein this salt bridge has been disrupted ($\alpha v_{R995D}\beta 3$ or $\alpha v\beta 3_{D723R}$). Further experiments were done in collaboration with Dr. Martina Müller, Clinical Research Unit, Dept. of Obstetrics & Gynecology, Technische Universität München.

We observed in transfected human ovarian cancer cells expressing an integrin αvβ3 variant which lacks the putative salt bridge, constitutive activation of integrin αvβ3-mediated signal transduction pathways and thus significantly increased OV-MZ-6 cancer cell proliferation. Moreover, integrin-related intracellular signaling molecules, such as the focal adhesion kinase (FAK), the mitogen-activated protein kinases (MAPK) $p44/42^{(erk-1/2)}$, and protein kinase B (PKB)/Akt, which are important for cell proliferation, were constitutively phosphorylated and thus activated (Müller et al., unpublished data). Those data support the hypothesis that disruption of a putative salt bridge in the cytoplasmic domain triggers integrin-related downstream signaling pathways, focal contact formation, and increased cell proliferation. This observation underlines the key role of the integrin salt bridge on integrin activation and integrin-mediated cell response. Our data are in line with the reports obtained by Hughes and co-workers from integrin αIIbβ3 (Hughes et al., 1996, 6571-6574, Imai et al., 2008, 5007-5015). They were the first to construct an integrin αIIbβ3 mutant in order to analyse the role of a putative cytoplasmic salt bridge between integrin α/β-subunits. For this, charge reversal point mutation in the salt bridge forming amino acid of integrin αIIbβ3 were generated. It was observed that salt bridge formation maintained the integrin in a resting and low-affinity state. Conversely, upon mutational disruption of the salt bridge, integrin "outside-in" signaling was constitutively activated (Hughes et al., 1996, 6571-6574).

In a similar way, Imai and co-workers disrupted the salt bridge by mutating the conserved cytoplasmic arginine in R^{GFFKR} in integrin α4 (Imai et al., 2008, 5007-5015). The authors investigated in an *in vivo* mouse model the role of this disrupted salt bridge on integrin α4β1 and α4β7 activation and ligand binding affinity. It was demonstrated that the disruption of the cytoplasmic membrane-proximal interaction leads to a constitutive activation and up-regulation of ligand binding affinity of integrin α4β1 and α4β7 (Imai et al., 2008, 5007-5015). Also these observations are in good agreement with our results and

that from Hughes and co-workers (Hughes et al., 1996, 6571-6574) since they support the hypothesis that salt bridge disruption results in a constitutively activated integrin capable of signaling and also promotion of cell proliferation.

However, as described above, there are conflicting results on the importance of salt bridge formation/disruption for integrin activation and integrin-mediated biological functions (Czuchra et al., 2006, 889-899). The mechanism of integrin activation was studied under physiological conditions in an *in vivo* transgenic mouse model which displayed the mutant $\beta1_{D759A}$. Since no obviously altered phenotype was observed, keratinocytes from these animals were *in vitro* expanded for their testing in cell biological assays. It turned out that β1-mediated cell adhesion, spreading, and migration were largely unaffected by the lack of salt bridge formation. Therefore the authors concluded that genetic disruption of the membrane-proximal salt bridge-mediated association did not provoke constitutive β1-activation (Czuchra et al., 2006, 889-899). However, NMR structure resolution for the integrin αIIbβ3 cytoplasmic domain showed that the salt bridge forming amino acid αIIb_{R995} does not only interact with the membrane-proximal $\beta3_{D723}$, but also with two other membrane-proximal conserved residues on the integrin β3-chain, $\beta3_{H722}$ and $\beta3_{E726}$. Therefore, it may be conceivable that the $\beta1_{D759A}$ perturbation of salt bridge formation in the *in vivo* mouse model might be at least partially compensated for by intact $\beta1_{H758}$ and/or $\beta1_{E762}$ (Imai et al., 2008, 5007-5015). Thereby, effects on integrin β1-provoked cell adhesion might only be weakly affected by the disruption of this salt bridge forming amino acids on the integrin β1 chain. As revealed by Hughes and co-workers, the cytoplasmic salt bridge interaction is an electrostatic connection which might be formed by more then one conserved residues within integrin α- and β-subunits.

Taken together, the issue of whether or what amino acids are directly and/or indirectly implicated in salt bridge or cytoplasmic interface formation is not fully resolved yet. This obscurity might explain the controversial results observed when studying the impact of the salt bridge on biological functions of integrin receptors in distinct *in vitro* and *in vivo* experimental model systems.

Furthermore, also other researchers described an integrin activation model in which the disruption of the integrin αIIbβ3 salt bridge by mutation of αIIb_{R995} and $\beta3_{D723}$ allowed the formation of a new salt bridge between the D723 of β3 and a specific lysine in the talin head domain (Anthis and Campbell, 2011, 191-198). Indeed, talin is known as an integrin activator due to its intracellular interaction with the β3 cytoplasmic domain (Takagi et al., 2002, 599-511, Calderwood, 2004, 657-666, Gahmberg et al., 2009, 431-444). This

inside-out activation of integrin allows cytoskeletal remodelling followed by the disruption of both, the interactions that exist between the transmembrane domains and also between the cytoplasmic tail of both integrin subunits (Takagi et al., 2002, 599-511, Calderwood, 2004, 657-666, Gahmberg et al., 2009, 431-444). Those data suggest that the putative salt bridge might not only be the direct actor in integrin receptor activation but might also play an indirect role in the connection of integrin receptor to intracellular activators, such as the head domain of the cytoskeletal protein talin.

4.3 Impact of the integrin αvβ3 transmembrane domain on human ovarian cancer cell proliferation

Integrins are known to be important for cell proliferation. The molecular mechanisms involved in cell proliferation include integrin-dependent activation of growth factor receptors, enhancement of growth factor signals, recruitment of crucial transducing proteins to membrane cytoskeletal complexes, increased MAPK activation, and enhancement of nuclear translocation of transcriptional regulators (Moro et al., 1998, 6622-6632). In tumor cells, adhesion-dependent control of cell proliferation is dysregulated (Vellon et al., 2005, 3759-3773). Integrin αvβ3 is involved in those cell pathological functions and thus has a critical role in tumor cell proliferation, adhesion, migration, and dissemination.

Hapke and co-workers observed that proliferation of human ovarian cancer cell lines OV-MZ-6 is under the control of integrin αvβ3 (Hapke et al., 2003, 1073-1083). The authors showed an increased adhesion and proliferation of OV-MZ-6 cancer cells associated with elevated integrin αvβ3 expression levels (Hapke et al., 2003, 1073-1083). In that regard, we were interested in investigating the role of the integrin αvβ3 TMD conformational states on OV-MZ-6 cancer cell proliferation. Integrin-TMD of both α- and β-subunits are supposed to share an electrostatic interaction highly similar to that observed for homodimerization of the TMD of GpA via the dimerization motif GxxxG. This association has been shown to be extremely stable (Senes et al., 2004, 465-479). In light of this, we generated expression vectors for integrin αvβ3 constructs in which, the complete TMD of the integrin αv- and the β3-subunit, respectively, was exchanged by the TMD of GpA. Molecular dynamic calculations had already suggested that GpA conformation might be energetically similar to the intermediate state of an integrin, where

both TMD are closely associated (Gottschalk, 2005, 703-712). Integrin αvβ3 TMD-GpA hybrid constructs served as a model for strong TMD-helical association. In addition, as control, we mutated the GxxxG dimerization motif to GxxxI which is known to abrogate TMD interaction of GpA (Lemmon et al., 1992, 7683-7689). In order to investigate the role of the integrin TMD conformation on integrin activation, OV-MZ-6 cells were stably transfected either to express an integrin αvβ3 TMD-GpA variant with strong TMD dimerization (TMD-GpA) or abrogated TMD dimerization (TMD-GpA-I). Then, the proliferative activity of both cell transfectants was analysed. In MTT assays and cell counting experiments, we observed markedly reduced proliferative activity of OV-MZ-6 cancer cells expressing TMD-GpA mutant compared to enhanced proliferative activity in those displaying the TMD-GpA-I mutant on their cell surfaces.

Recently, Zhu and co-workers performed crosslinking studies of the TMD of a similar chimera of integrin αIIbβ3 with a GpA-TMD and found a crosslinking pattern compatible with a GpA-like conformation (Zhu et al., 2009, 234-249). The authors found out that substitution of the integrin αIIbβ3-TMD by the GpA-TMD results in low-affinity activation state of the integrin which is due to the strong GpA-TMD association (Zhu et al., 2009, 234-249). However, the conformation of the GpA-TMD chimera was shown to be modified compared to the TMD of the wild type integrin. The rotational orientation of the integrin β3-subunit was changed by approximately 100° followed by a modification of the tilt angle between both integrin TMD helices (Gottschalk et al., 2002, 1800-1812). This conformational rearrangement is thought to disrupt the cytoplasmic interaction formed by a putative salt bridge which maintains the integrin in a resting, low-affinity state. Deletion of this contact might facilitate the transformation from a closed, inactive integrin conformation to an active, open, high-affinity state (Hughes et al., 1996, 6571-6574, Vinogradova et al., 2002, 587-597, Lau et al., 2009, 1351-1361).

Based on those data, Müller and co-workers investigated the impact of integrin TMD clasping/unclasping constructs on integrin-mediated cell signaling. Protein kinase B (PKB)/Akt and mitogen activated protein kinase (MAPK) are important cell signaling proteins and are mandatory for inducing cellular proliferative response. Hence, Müller and co-workers found significantly increased activation of both cell signaling proteins by cells expressing TMD-GpA-I compared to cells expressing TMD-GpA with impaired signaling capability (Müller et al, unpublished data).

Hence, our hypothesis is that TMD-GpA chimera presents the characteristics of an intermediate integrin activation state occurring right after inside-out signaling but before

outside-in signaling (Müller et al., unpublished data). The existence of such an intermediate primed state has been previously suggested by Alon and co-workers when analyzing the effect of chemokines on integrin α4β1 (Alon and Dustin, 2007, 17-27). The authors observed that this intermediate state of the integrin needs engagement by an ECM ligand as well as the presence of forces for further activation, observations which are in good agreement with our data.

4.4 Epidermal growth factor receptor expression as a function of the integrin αvβ3 transmembrane domain conformation

Cell proliferation, migration, and survival are important cell tasks regulated by a large number of factors such as cell/ECM, cell/cell interactions, nutrients, and growth factors interacting with their respective receptors. Carcinogenesis leads to a destabilisation of those interactions and to cancer cells that escape the control of normal growth. Integrins are known to be involved in all of those cell biological functions, requiring the interaction with other molecules, such as growth factors and their receptors (Lössner et al., 2008, 2746-2761).

Lössner and co-workers showed that epidermal growth factor receptor (EGF-R) expression in human OV-MZ-6 ovarian cancer cells is under the control of integrin αvβ3 (Lössner et al., 2008, 2746-2761). They observed that elevated integrin αvβ3 expression levels resulted in a significant upregulation of EGF-R expression as well as its phosphorylated and thus activated form, p-EGF-R, compared to vector-transfected and wild type cells which both display low endogenous integrin αvβ3 expression. However, the precise mechanism by which integrins influence growth factor receptor expression is not yet full understood. Based on these previous findings of our group, we were interested to analyse the contribution of the integrin αvβ3 TMD conformation and thus the integrin activation state on (p-)EGF-R expression. Our data revealed significantly elevated p-EGF-R/EGF-R expression in cells carrying the TMD-GpA mutant compared to cells expressing integrin αvβ3 wild type. In contrast, OV-MZ-6 cells expressing a fully active integrin αvβ3 (TMD-GpA-I) did not exhibit significant elevation of p-EGF-R/EGF-R protein. Therefore, it might be speculated that cells with an impaired signaling and proliferative response through the expression of the TMD-GpA mutants, might compensate their inability to integrin-mediated signaling and proliferation by increasing other signaling

pathway via EGF-R. On the contrary, the full and constitutive activation of integrin αvβ3 (TMD-GpA-I), might not longer depend on strong integrin/EGF-R crosstalk for full proliferative cell response.

Our results are in line with the results obtained by Lössner and co-workers, revealing that overexpression of integrin αvβ3 in human ovarian OV-MZ-6 cancer cells resulted in a modification and upregulation of p-EGF-R/EGF-R protein expression. This is however, in contrast to other findings, revealing that other integrin receptor such as α6β4 did not alter total EGF-R expression level (Yoon et al., 2006, 2732-2739). Opposite effects have also been reported concerning the impact of integrins on the EGF-R protein. In that respect, Mattila and co-workers showed that integrin α1β1 acts as a negative regulator on EGF-R signaling by reducing EGF-R phosphorylation and thus its activation (Mattila et al., 2005, 78-85).

These conflicting results obtained by different studies might possibly arise from the use of different integrins, growth factor receptors, and the type of cells studied. Nevertheless, it appears very important to comprehend the crosstalk that exists between integrins and EGF-R signaling pathway and how those signals are integrated in cell biological functions.

As already mentioned herein above, integrin αvβ3 and EGF are known to be involved in malignant ovarian cancer cell progression (Hapke et al., 2003, 1073-1083, Lössner et al., 2008, 2746-2761). Although there is a large amount of studies regarding the signaling pathways activated by both integrin and growth factor receptors, little is known about how those signals are integrated and synchronized for cell biological functions. Lössner and co-workers showed that the proliferative response of human ovarian OV-MZ-6 cancer cells upon EGF stimulation is increased by cells with elevated integrin αvβ3 level compared to cells with low endogenous αvβ3 expression level (Lössner et al., 2008, 2746-2761). Those observations and together with ours (see 3.4.1) regarding the influence of integrin αvβ3-TMD mutants on EGF-R expression, lead us to investigate the effect of one EGF, ligand of the EGF-R, on the proliferative activity of human ovarian cancer cells transfected to express different integrin αvβ3-TMD mutants. In preliminary studies, to our surprise we did not detect any significant difference in the proliferative activity of all different OV-MZ-6 cell transfectants upon EGF stimulation even if the EGF-R expression level varied from one model to another. The fact that the presence of EGF did not induce an increase of the proliferative response of ovarian cancer cells transfected to express wild type integrin αvβ3 as it was already demonstrated by Lössner and co-workers (Lössner et

al., 2008, 2746-2761) indicates that the culture conditions of those experiments were not optimized and need further future experimental work. Moreover, other ligands for the EGF-R, such as transforming growth factor-α (TGF-α) or amphiregulin, have to be tested with respect to their effect on EGF-R ligation.

4.5 Summary

Integrin αvβ3 is involved in one of the most malignant and therapy-resistant diseases, human ovarian cancer. The primary tumor is highly aggressive, ovarian cancer cells adhere, migrate, and proliferate fast, resulting in an early intraperitoneal metastatic development/dissemination. Metastasis is the leading cause of high morbidity and mortality in ovarian cancer. Angiogenesis is essential for cancer progression and metastatic cell dissemination. Integrin αvβ3 is known as one of the active mediators in angiogenesis (Zhaofei Liu, 2008, 329–339), tumor invasion and metastasis (Somanath et al., 2009, 177-185, Streuli and Akhtar, 2009, 491-506) and has evolved into a prime target molecule for anti-cancer drugs (Arndt et al., 2005, 93-141).

The aim of the present dissertation was to generate integrin αvβ3 cytoplasmic and transmembrane domain mutants by *in vitro* site-directed mutagenesis.

1) For studies aiming at elucidating the role of integrin TMD clasping/unclasping for integrin activation, the following TMD mutants were generated, i.e. TMD-GpA (clasped TMD dimerization) and TMD-GpA-I (unclasped TMD dimerization).

2) The role of a putative cytoplasmic salt bridge for integrin activation was pursued by generating mutants of integrin αvβ3 in which the salt bridge forming amino acids were mutually exchanged (αv_{R995D}; $\beta 3_{D723R}$). OV-MZ-6 cells were transfected to express αvβ3 integrins either capable to form a putative salt bridge or wherein this salt bridge has been disrupted.

Functionally, the following studies were done in the present work:

a) We studied the effect of the two integrin TMD variants on one cell biological aspect, the proliferative activity of OV-MZ-6 cancer cells. TMD-GpA cell transfectants showed weaker cell proliferative activity, whereas TMD-GpA-I cell transfectants were detected with strongly enhanced cell proliferation. This demonstrates that, integrin function can be allosterically finely-tuned through the integrin TMD. Wild type integrins have a high plasticity in adopting different states, while TMD-GpA arrest the integrin in

an intermediate state and TMD-GpA-I in a constitutively fully activated state. Hence, the TMD sequence in various integrins may be functionally important.

b) We analysed the contribution of integrin αvβ3 TMD conformation on growth factor receptor expression, knowing that the integrin αvβ3 induce changes in expression and activity of growth factor receptor (Lössner et al., 2008, 2746-2761). We observed significantly increased p-EGF-R/EGF-R expression in cells carrying TMD-GpA mutant. In contrast, TMD-GpA-I displaying an constitutively activated integrin state did not significantly affect p-EGF-R/EGF-R expression levels. The exact mechanisms of the regulation of EGF-R expression and activation as a function of the integrin αvβ3 activation state is subject of current investigations.

The present work demonstrated that an integrin αvβ3 with a clasped TMD (TMD-GpA), which represents a "primed" intermediate integrin conformation, is fully capable of ligand binding but restrained in intracellular signal transduction. However, mutation of the integrin TMD that results in an open conformation (TMD-GpA-I) is accompanied by constitutive activation of the receptor allowing signaling and as a consequence, cell biological effects which are based on signal transduction, such as cell proliferation. Thus, with the two TMD constructs we were able to decouple integrin-mediated cellular adhesive capacity from signaling.

Our understanding of the mechanism of alterations of conformational states during integrin activation will be of great importance for the development of specific integrin αvβ3 allosteric antagonists. The understanding of TMD/cytoplasmic conformational states during integrin activation will thus facilitate future therapeutical approaches for targeting integrins by the design of allosteric inhibitors capable of locking integrins in an inactivated state.

5 List of figures

6 References

Adair, B. D. X., J. P. Maddock, C. Goodman, S. L. Arnaout, M. A. Yeager, M. (2005). "Three-dimensional EM structure of the ectodomain of integrin {alpha}V{beta}3 in a complex with fibronectin." J Cell Biol **168**(7): 1109-1118

Al-Jamal, R. and Harrison, D. J. (2008). "Beta1 integrin in tissue remodelling and repair: from phenomena to concepts." Pharmacol Ther **120**(2): 81-101

Albelda, S. M., Mette, S. A., Elder, D. E., Stewart, R., Damjanovich, L., Herlyn, M. and Buck, C. A. (1990). "Integrin distribution in malignant melanoma: association of the beta 3 subunit with tumor progression." Cancer Res **50**(20): 6757-6764

Alon, R. and Dustin, M. L. (2007). "Force as a facilitator of integrin conformational changes during leukocyte arrest on blood vessels and antigen-presenting cells." Immunity **26**(1): 17-27

Anthis, N. J. and Campbell, I. D. (2011). "The tail of integrin activation." Trends Biochem Sci **36**(4): 191-198

Anthis, N. J., Haling, J. R., Oxley, C. L., Memo, M., Wegener, K. L., Lim, C. J., Ginsberg, M. H. and Campbell, I. D. (2009). "Beta integrin tyrosine phosphorylation is a conserved mechanism for regulating talin-induced integrin activation." J Biol Chem **284**(52): 36700-36710

Arndt, T., Arndt,U, Reuning, U, Kessler,H (2005). Cancer therapy : molecular targets in tumor-host interactions, Chapter 7: Integrins in Angiogenesis: Implications for Tumor Therapy

Beekman, K. W., Colevas, A. D., Cooney, K., Dipaola, R., Dunn, R. L., Gross, M., Keller, E. T., Pienta, K. J., Ryan, C. J., Smith, D. and Hussain, M. (2006). "Phase II evaluations of cilengitide in asymptomatic patients with androgen-independent prostate cancer: scientific rationale and study design." Clin Genitourin Cancer **4**(4): 299-302

Bello, L., Francolini, M., Marthyn, P., Zhang, J., Carroll, R. S., Nikas, D. C., Strasser, J. F., Villani, R., Cheresh, D. A. and Black, P. M. (2001). "Alpha(v)beta3 and alpha(v)beta5 integrin expression in glioma periphery." Neurosurgery **49**(2): 380-389; discussion 390
Bennett, J. S., Berger, B. W. and Billings, P. C. (2009). "The structure and function of platelet integrins." J Thromb Haemost **7 Suppl 1**: 200-205

Boettiger, D., Huber, F., Lynch, L. and Blystone, S. (2001). "Activation of alpha(v)beta3-vitronectin binding is a multistage process in which increases in bond strength are dependent on Y747 and Y759 in the cytoplasmic domain of beta3." Mol Biol Cell **12**(5): 1227-1237

Bosserhoff, A.-K. (2006). Expert Opinion on Therapeutic Patents, Juli 2006, Vol. 16, No 7 :Integrins as targets in therapy (963-975). Regensburg

Bunch, T. A. (2010). "Integrin alphaIIbbeta3 activation in Chinese hamster ovary cells and platelets increases clustering rather than affinity." J Biol Chem **285**(3): 1841-1849

Cabodi, S., Moro, L., Bergatto, E., Boeri Erba, E., Di Stefano, P., Turco, E., Tarone, G. and Defilippi, P. (2004). "Integrin regulation of epidermal growth factor (EGF) receptor and of EGF-dependent responses." Biochem Soc Trans **32**(Pt3): 438-442

Calderwood, D. A. (2004). "Integrin activation." J Cell Sci **117**(Pt 5): 657-666

Cruet-Hennequart, S., Maubant, S., Luis, J., Gauduchon, P., Staedel, C. and Dedhar, S. (2003). "alpha(v) integrins regulate cell proliferation through integrin-linked kinase (ILK) in ovarian cancer cells." Oncogene **22**(11): 1688-1702

Czuchra, A., Meyer, H., Legate, K. R., Brakebusch, C. and Fassler, R. (2006). "Genetic analysis of beta1 integrin "activation motifs" in mice." J Cell Biol **174**(6): 889-899

Desgrosellier, J. S. C., D. A. (2010). "Integrins in cancer: biological implications and therapeutic opportunities." Nat Rev Cancer **10**(1): 9-22

Eliceiri, B. P. and Cheresh, D. A. (1998). "The role of alphav integrins during angiogenesis." Mol Med **4**(12): 741-750

Gahmberg, C. G., Fagerholm, S. C., Nurmi, S. M., Chavakis, T., Marchesan, S. and Gronholm, M. (2009). "Regulation of integrin activity and signalling." Biochim Biophys Acta **1790**(6): 431-444

Giancotti, F. G. (1997). "Integrin signaling: specificity and control of cell survival and cell cycle progression." Curr Opin Cell Biol **9**(5): 691-700

Gottschalk, K. E. (2005). "A coiled-coil structure of the alphaIIbbeta3 integrin transmembrane and cytoplasmic domains in its resting state." Structure **13**(5): 703-712

Gottschalk, K. E., Adams, P. D., Brunger, A. T. and Kessler, H. (2002). "Transmembrane signal transduction of the alpha(IIb)beta(3) integrin." Protein Sci **11**(7): 1800-1812

Gottschalk, K. E. and Kessler, H. (2004). "A computational model of transmembrane integrin clustering." Structure **12**(6): 1109-1116

Hapke, S., Kessler, H., Arroyo de Prada, N., Benge, A., Schmitt, M., Lengyel, E. and Reuning, U. (2001). "Integrin alpha(v)beta(3)/vitronectin interaction affects expression of the urokinase system in human ovarian cancer cells." J Biol Chem **276**(28): 26340-26348

Hapke, S., Kessler, H., Luber, B., Benge, A., Hutzler, P., Hofler, H., Schmitt, M. and Reuning, U. (2003). "Ovarian cancer cell proliferation and motility is induced by engagement of integrin alpha(v)beta3/Vitronectin interaction." Biol Chem **384**(7): 1073-1083

Harburger, D. S. and Calderwood, D. A. (2009). "Integrin signalling at a glance." J Cell Sci **122**(Pt 2): 159-163

Hardjasa, A., Ling, M., Ma, K., and Yu, H. (2010). "Investigating the Effects of DMSO on PCR Fidelity Using a Restriction Digest-Based Method." Journal of Experimental Microbiology and Immunology (JEMI) **Vol. 14**: 161-164

Harms, J. F., Welch, D. R., Samant, R. S., Shevde, L. A., Miele, M. E., Babu, G. R., Goldberg, S. F., Gilman, V. R., Sosnowski, D. M., Campo, D. A., Gay, C. V., Budgeon, L. R., Mercer, R., Jewell, J., Mastro, A. M., Donahue, H. J., Erin, N., Debies, M. T., Meehan, W. J., Jones, A. L., Mbalaviele, G., Nickols, A., Christensen, N. D., Melly, R., Beck, L. N., Kent, J., Rader, R. K., Kotyk, J. J., Pagel, M. D., Westlin, W. F. and Griggs, D. W. (2004). "A small molecule antagonist of the alpha(v)beta3 integrin suppresses MDA-MB-435 skeletal metastasis." Clin Exp Metastasis **21**(2): 119-128

Hermann, P., Armant, M., Brown, E., Rubio, M., Ishihara, H., Ulrich, D., Caspary, R. G., Lindberg, F. P., Armitage, R., Maliszewski, C., Delespesse, G. and Sarfati, M. (1999). "The vitronectin receptor and its associated CD47 molecule mediates proinflammatory cytokine synthesis in human monocytes by interaction with soluble CD23." J Cell Biol **144**(4): 767-775

Hoefling, M., Kessler, H. and Gottschalk, K. E. (2009). "The transmembrane structure of integrin alphaIIbbeta3: significance for signal transduction." Angew Chem Int Ed Engl **48**(36): 6590-6593

Horton, M. A. (1997). "The alpha v beta 3 integrin "vitronectin receptor"." Int J Biochem Cell Biol **29**(5): 721-725

Hughes, P. E., Diaz-Gonzalez, F., Leong, L., Wu, C., McDonald, J. A., Shattil, S. J. and Ginsberg, M. H. (1996). "Breaking the integrin hinge. A defined structural constraint regulates integrin signaling." J Biol Chem **271**(12): 6571-6574

Humphries, J. D., Byron, A. and Humphries, M. J. (2006). "Integrin ligands at a glance." J Cell Sci **119**(Pt 19): 3901-3903

Humphries, M. J. (2000). "Integrin structure." Biochem Soc Trans **28**(4): 311-339

Hynes, R. O. (2002). "Integrins: bidirectional, allosteric signaling machines." Cell **110**(6): 673-687

Imai, Y., Park, E. J., Peer, D., Peixoto, A., Cheng, G., von Andrian, U. H., Carman, C. V. and Shimaoka, M. (2008). "Genetic perturbation of the putative cytoplasmic membrane-proximal salt bridge aberrantly activates alpha(4) integrins." Blood **112**(13): 5007-5015

Jorissen, R. N., Walker, F., Pouliot, N., Garrett, T. P., Ward, C. W. and Burgess, A. W. (2003). "Epidermal growth factor receptor: mechanisms of activation and signalling." Exp Cell Res **284**(1): 31-53

Kim, D. S., Jeon, O. H., Lee, H. D., Yoo, K. H. and Kim, D. S. (2008). "Integrin alphavbeta3-mediated transcriptional regulation of TIMP-1 in a human ovarian cancer cell line." Biochem Biophys Res Commun **377**(2): 479-483

Kim, M., Carman, C. V. and Springer, T. A. (2003). "Bidirectional transmembrane signaling by cytoplasmic domain separation in integrins." Science **301**(5640): 1720-1725

Lau, T. L., Kim, C., Ginsberg, M. H. and Ulmer, T. S. (2009). "The structure of the integrin alphaIIbbeta3 transmembrane complex explains integrin transmembrane signalling." Embo J **28**(9): 1351-1361

Le Tourneau, C., Faivre, S. and Raymond, E. (2007). "The role of integrins in colorectal cancer." Oncology (Williston Park) **21**(9 Suppl 3): 21-24

Lemmon, M. A., Flanagan, J. M., Hunt, J. F., Adair, B. D., Bormann, B. J., Dempsey, C. E. and Engelman, D. M. (1992). "Glycophorin A dimerization is driven by specific interactions between transmembrane alpha-helices." J Biol Chem **267**(11): 7683-7689

Li, R., Babu, C. R., Lear, J. D., Wand, A. J., Bennett, J. S. and DeGrado, W. F. (2001). "Oligomerization of the integrin alphaIIbbeta3: roles of the transmembrane and cytoplasmic domains." Proc Natl Acad Sci U S A **98**(22): 12462-12467

Li, R., Gorelik, R., Nanda, V., Law, P. B., Lear, J. D., DeGrado, W. F. and Bennett, J. S. (2004). "Dimerization of the transmembrane domain of Integrin alphaIIb subunit in cell membranes." J Biol Chem **279**(25): 26666-26673

Liapis, H., Adler, L. M., Wick, M. R. and Rader, J. S. (1997). "Expression of alpha(v)beta3 integrin is less frequent in ovarian epithelial tumors of low malignant potential in contrast to ovarian carcinomas." Hum Pathol **28**(4): 443-449

Lössner, D., Abou-Ajram, C., Benge, A., Aumercier, M., Schmitt, M. and Reuning, U. (2009). "Integrin alphavbeta3 upregulates integrin-linked kinase expression in human ovarian cancer cells via enhancement of ILK gene transcription." J Cell Physiol **220**(2): 367-375

Lössner, D., Abou-Ajram, C., Benge, A. and Reuning, U. (2008). "Integrin alphavbeta3 mediates upregulation of epidermal growth-factor receptor expression and activity in human ovarian cancer cells." Int J Biochem Cell Biol **40**(12): 2746-2761

Luo, B. H., Carman, C. V. and Springer, T. A. (2007). "Structural basis of integrin regulation and signaling." Annu Rev Immunol **25**: 619-647

Luo, B. H. and Springer, T. A. (2006). "Integrin structures and conformational signaling." Curr Opin Cell Biol **18**(5): 579-586

Luo, B. H., Springer, T. A. and Takagi, J. (2004). "A specific interface between integrin transmembrane helices and affinity for ligand." PLoS Biol **2**(6): e153

Mattila, E., Pellinen, T., Nevo, J., Vuoriluoto, K., Arjonen, A. and Ivaska, J. (2005). "Negative regulation of EGFR signalling through integrin-alpha1beta1-mediated activation of protein tyrosine phosphatase TCPTP." Nat Cell Biol **7**(1): 78-85

Mobus, V., Gerharz, C. D., Press, U., Moll, R., Beck, T., Mellin, W., Pollow, K., Knapstein, P. G. and Kreienberg, R. (1992). "Morphological, immunohistochemical and biochemical characterization of 6 newly established human ovarian carcinoma cell lines." Int J Cancer **52**(1): 76-84

Morgan, M. R., Byron, A., Humphries, M. J. and Bass, M. D. (2009). "Giving off mixed signals--distinct functions of alpha5beta1 and alphavbeta3 integrins in regulating cell behaviour." IUBMB Life **61**(7): 731-738

Moro, L., Dolce, L., Cabodi, S., Bergatto, E., Boeri Erba, E., Smeriglio, M., Turco, E., Retta, S. F., Giuffrida, M. G., Venturino, M., Godovac-Zimmermann, J., Conti, A., Schaefer, E., Beguinot, L., Tacchetti, C., Gaggini, P., Silengo, L., Tarone, G. and Defilippi, P. (2002). "Integrin-induced epidermal growth factor (EGF) receptor activation requires c-Src and p130Cas and leads to phosphorylation of specific EGF receptor tyrosines." J Biol Chem **277**(11): 9405-9414

Moro, L., Venturino, M., Bozzo, C., Silengo, L., Altruda, F., Beguinot, L., Tarone, G. and Defilippi, P. (1998). "Integrins induce activation of EGF receptor: role in MAP kinase induction and adhesion-dependent cell survival." Embo J **17**(22): 6622-6632

Partridge, A. W., Liu, S., Kim, S., Bowie, J. U. and Ginsberg, M. H. (2005). "Transmembrane domain helix packing stabilizes integrin alphaIIbbeta3 in the low affinity state." J Biol Chem **280**(8): 7294-7300

Primose S., T. R. (2006). Principles of Gene Manipulation and Genomics, 8. Changing Genes: Site-directed Mutagenesis and Protein Engineering, 141-156

Schneider, D. and Engelman, D. M. (2004). "Involvement of transmembrane domain interactions in signal transduction by alpha/beta integrins." J Biol Chem **279**(11): 9840-9846

Senes, A., Engel, D. E. and DeGrado, W. F. (2004). "Folding of helical membrane proteins: the role of polar, GxxxG-like and proline motifs." Curr Opin Struct Biol **14**(4): 465-479

Somanath, P. R., Malinin, N. L. and Byzova, T. V. (2009). "Cooperation between integrin alphavbeta3 and VEGFR2 in angiogenesis." Angiogenesis **12**(2): 177-185

Streuli, C. H. and Akhtar, N. (2009). "Signal co-operation between integrins and other receptor systems." Biochem J **418**(3): 491-506

Takagi, J., Petre, B. M., Walz, T. and Springer, T. A. (2002). "Global conformational rearrangements in integrin extracellular domains in outside-in and inside-out signaling." Cell **110**(5): 599-511

Tamkun JW, DeSimone DW, Fonda D, Patel RS, Buck C, Horwitz AF, Hynes RO. (1986). "Structure of integrin, a glycoprotein involved in the transmembrane linkage between fibronectin and actin." Cell **46**(2):271-282

Travis, M. A., Humphries, J. D. and Humphries, M. J. (2003). "An unraveling tale of how integrins are activated from within." Trends Pharmacol Sci **24**(4): 192-197

Veeravagu, A., Liu, Z., Niu, G., Chen, K., Jia, B., Cai, W., Jin, C., Hsu, A. R., Connolly, A. J., Tse, V., Wang, F. and Chen, X. (2008). "Integrin alphavbeta3-targeted radioimmunotherapy of glioblastoma multiforme." Clin Cancer Res **14**(22): 7330-7339

Vellon, L., Menendez, J. A. and Lupu, R. (2005). "AlphaVbeta3 integrin regulates heregulin (HRG)-induced cell proliferation and survival in breast cancer." Oncogene **24**(23): 3759-3773

Vinogradova, O., Velyvis, A., Velyviene, A., Hu, B., Haas, T., Plow, E. and Qin, J. (2002). "A structural mechanism of integrin alpha(IIb)beta(3) "inside-out" activation as regulated by its cytoplasmic face." Cell **110**(5): 587-597

Watt, F. M. (2002). "Role of integrins in regulating epidermal adhesion, growth and differentiation." Embo J **21**(15): 3919-3926

Wilder, R. L. (2002). "Integrin alpha V beta 3 as a target for treatment of rheumatoid arthritis and related rheumatic diseases." Ann Rheum Dis **61 Suppl 2**: 96-99

Xiong, J. P., Stehle, T., Diefenbach, B., Zhang, R., Dunker, R., Scott, D. L., Joachimiak, A., Goodman, S. L. and Arnaout, M. A. (2001). "Crystal structure of the extracellular segment of integrin alpha Vbeta3." Science **294**(5541): 339-345

Xiong, J. P., Stehle, T., Zhang, R., Joachimiak, A., Frech, M., Goodman, S. L. and Arnaout, M. A. (2002). "Crystal structure of the extracellular segment of integrin alpha Vbeta3 in complex with an Arg-Gly-Asp ligand." Science **296**(5565): 151-155

Yang, J., Ma, Y. Q., Page, R. C., Misra, S., Plow, E. F. and Qin, J. (2009). "Structure of an integrin alphaIIb beta3 transmembrane-cytoplasmic heterocomplex provides insight into integrin activation." Proc Natl Acad Sci U S A **106**(42): 17729-17734

Yoon, S. O., Shin, S. and Lipscomb, E. A. (2006). "A novel mechanism for integrin-mediated ras activation in breast carcinoma cells: the alpha6beta4 integrin regulates ErbB2 translation and transactivates epidermal growth factor receptor/ErbB2 signaling." Cancer Res **66**(5): 2732-2739

Zhaofei Liu, F. W., Xiaoyuan Chen (2008). Drug Development Research, Integrin αvβ3-targeted cancer therapy:Volume 69, Issue 6, 285–372

Zhu, J., Carman, C. V., Kim, M., Shimaoka, M., Springer, T. A. and Luo, B. H. (2007). "Requirement of alpha and beta subunit transmembrane helix separation for integrin outside-in signaling." Blood **110**(7): 2475-2483

Zhu, J., Luo, B. H., Barth, P., Schonbrun, J., Baker, D. and Springer, T. A. (2009). "The structure of a receptor with two associating transmembrane domains on the cell surface: integrin alphaIIbbeta3." Mol Cell **34**(2): 234-249

Zhu, J., Luo, B. H., Xiao, T., Zhang, C., Nishida, N. and Springer, T. A. (2008). "Structure of a complete integrin ectodomain in a physiologic resting state and activation and deactivation by applied forces." Mol Cell **32**(6): 849-861

Acknowledgement

In the first place, I would like to extend my warmest thanks to Prof. Dr. Ute Reuning for excellent guidance and supervision during this work, as well as for giving me the opportunity to work on this project. I also would like to express my gratitude for her being always available for questions, spending a lot of time for discussions and correcting my doctor thesis.

I would like to thank Prof. Dr. Manfred Schmitt and all the members of the Clinical Research Group (Department of Obstetrics and Gynecology, Klinikum rechts der Isar, Technische Universität München) for their advice and technical assistance. I will always be glad to remember our time shared. In particular, I would like to thank Mrs. Anke Benge for the pleasant times together in the laboratory and for accompanying me in all phases of this extended project; of course, not to forget our colleagues Martina Müller, Lilli Volkhardt, Bettina Grismayer, Alexandra Stöckel and Haissi Cui. I am glad to have made your acquaintance.

I am very grateful for the support of Patrice Hermann, spending a lot of time correcting my work, being open for my questions and very patient for discussions.

I would like to dedicate this work to my dauther and my husband, who always listened to me and supported me, as well as to my parents and my brother, who continuously encouraged me throughout my time of education.